



HAL
open science

Newton time-extracting wavelet transform: an effective tool for characterizing frequency-varying signals with weakly-separated components and theoretical analysis

Wenting Li, François Auger, Zhuosheng Zhang, Xiangxiang Zhu

► To cite this version:

Wenting Li, François Auger, Zhuosheng Zhang, Xiangxiang Zhu. Newton time-extracting wavelet transform: an effective tool for characterizing frequency-varying signals with weakly-separated components and theoretical analysis. *Signal Processing*, 2023, 10.1016/j.sigpro.2023.109017 . hal-04039414

HAL Id: hal-04039414

<https://hal.science/hal-04039414>

Submitted on 21 Mar 2023

HAL is a multi-disciplinary open access archive for the deposit and dissemination of scientific research documents, whether they are published or not. The documents may come from teaching and research institutions in France or abroad, or from public or private research centers.

L'archive ouverte pluridisciplinaire **HAL**, est destinée au dépôt et à la diffusion de documents scientifiques de niveau recherche, publiés ou non, émanant des établissements d'enseignement et de recherche français ou étrangers, des laboratoires publics ou privés.

Newton time-extracting wavelet transform: an effective tool for characterizing frequency-varying signals with weakly-separated components and theoretical analysis

Wenting Li^a, François Auger^b, Zhuosheng Zhang^{a,*}, Xiangxiang Zhu^c

^a*School of Mathematics and Statistics, Xi'an Jiaotong University, 710049 Xi'an, China*

^b*Institut de Recherche en Énergie Électrique de Nantes Atlantique (IREENA, UR 4642), Nantes Université, Saint-Nazaire, France*

^c*School of Mathematics and Statistics, Northwestern Polytechnical University, 710049 Xi'an, China*

Abstract

In this paper, we propose a high resolution time-frequency (TF) analysis method called Newton time-extracting wavelet transform (NTEWT), which is designed to analyze frequency-varying signals with fast varying group delay (GD). Firstly, we discuss the relationship among the fixed points of time reassignment operator, the ridge points of wavelet transform and GD of the signal. Combining the above relations and Newton algorithm, we propose a Newton GD estimator. By only retaining the TF information most related to frequency-varying features of the signal and removing the weakly-related TF coefficients, we further introduce the NTEWT, which can not only achieve a more concentrated TF representation, but also enable signal reconstruction. Meanwhile, we develop a theoretical analysis of NTEWT under the mathematical framework. Firstly, we introduce a precise mathematical definition of a class of weakly-separated frequency-varying chirp-like components, and we prove that Newton GD estimator can accurately estimate GD of arbitrary function in this class, and NTEWT does indeed succeed in decomposing these functions. Finally, we use numerical experiments to evaluate the performance of the proposed NTEWT in terms of TF concentration, GD estimation and signal reconstruction.

Keywords: Time-frequency analysis, Time reassignment operator, Group delay, Ridge, Newton time-extracting wavelet transform, Signal reconstruction

1. Introduction

Non-stationary signals widely appear in various fields, such as radar and sonar [1, 2], seismic [3], biomedicine [4, 5], and mechanical engineering [6, 7], etc. Time-frequency analysis (TFA) can convert one-dimensional signals into two-dimensional time-frequency (TF) representations (TFR) efficiently, which helps to detect the TF feature of non-stationary signals in the TF plane visually [8, 9]. Many effective TFA methods mainly include linear TFA methods, nonlinear TFA methods and bilinear TFA methods. Linear TFA methods, such as the short-time Fourier transform (STFT) [8] and the wavelet transform

*Corresponding author.

Email address: zszhang@mail.xjtu.edu.cn (Zhuosheng Zhang)

(WT) [9], calculate the inner product between the signal and the basis function to characterize the TF structure of signal. Generally, the better the basis function matches the signal, the more suitable it is to characterize TF features with concentrated energy. Nonlinear TFA methods aim to construct new basis functions to characterize the non-linearity of signals, such as linear chirplet transform [10], local polynomial transform [11], and matched demodulation transform [12], etc. However, restricted by the Heisenberg uncertainty principle, linear and nonlinear TFA methods often generate blurry TFRs, and they had difficulty providing accurate TF descriptions for signals. Besides, bilinear TFA methods, such as the Wigner-Ville distribution [1] and its variants, which can effectively improve the TF resolution of mono-component signals, but introduce interference terms for multi-component signals and thus reduce the readability of the TFRs. In order to overcome these shortcomings, some advanced methods have been proposed successively.

The reassignment method (RM), proposed by Kodera et al. to the spectrogram [13, 14], and generalized by Auger and Flandrin to any bilinear time-frequency or time-scale distribution [15], is an old but under-explored method [16, 17, 18]. In parallel, Daubechies and Maes proposed the synchrosqueezing wavelet transform (SWT) [19] based on a phase technique to analyse auditory signals, which is a special case of the RM. And Huang et al. introduced an empirical mode decomposition (EMD) [20] to decompose the signal into a series of intrinsic mode functions in a data-driven manner. Though attractive because of its effectiveness and simplicity [21, 22], EMD lacks solid mathematical foundations. In this context, SWT has resurfaced as an alternative theoretical way to understand the principle of EMD with a convenient mathematical framework [23]. RM has, in turn, received new attention [24-26]. Although the RM relocates TF energy aiming to sharpen the TFR, and employs instantaneous frequency (IF) and group delay (GD) estimators, it is not invertible unfortunately. While SWT can reconstruct the interesting signals but suffers from blurred TFRs for signals with fast varying IF. Furthermore, new extensions of SWT have been developed [7, 27-32], among these improved methods, recently synchroextracting transform (SET) [32] has attracted great attention. Differing from the squeezing manner of SWT, SET only utilizes a small number of TF coefficients, but achieves a more concentrated TFR. Similar to SWT, SET also develops the corresponding higher-order extensions [33-35].

On the one hand, based on different features of signals, signals are divided into time-varying signals and frequency-varying signals. The TF energy distribution of time-varying signals spread around the IF trajectory, which can help to better identify the variation law of time-varying signals along the time direction, while the TF energy distribution of frequency-varying signals spread around the GD trajectory, which can effectively reflect the variation law of frequency-varying signals along the frequency direction. On the other hand, according to different direction of post-processing, TFA post-processing methods are divided into three categories. The first class considers both time and frequency directions, such as reassigned scalogram (RS), although RS can improve both the time resolution and the frequency/scale resolution of the TFR, unfortunately, it cannot reconstruct the signal. The second class considers only

frequency direction, such as SWT [23], matching synchrosqueezing wavelet transform (MSWT) [7], SET [32] and self-matched extracting wavelet transform (SMEWT) [34]. These TFA methods can reconstruct signals, and they are more suitable for characterizing slowly or strongly time-varying signals, but they may be no longer applicable for characterizing frequency-varying signals. In order to accurately analyze frequency varying signals, the third class of TFA post-processing along the time direction have emerged, including the time-reassigned synchrosqueezing transform (TSST) [36] and transient-extracting transform (TET) [37], and our recently proposed time-reassigned synchrosqueezing wavelet transform (TSWT) [38] and time-extracting wavelet transform (TEWT) [39], where we provide rigorous theoretical analysis of TSWT and TEWT for frequency-varying signals under the mathematical framework. Moreover, second-order TSST (TSST2) [40, 41] and second-order TET [42, 43] have been proposed. Indeed, these TFA methods reassigning or extracting along the time direction can reconstruct signals and are suitable for characterizing slowly or strongly frequency-varying signals.

It can be concluded that one of the advantages of TET/TEWT is to extract the TF coefficients of the fixed points of time reassignment operator, because the time reassignment operator can accurately estimate the GD of impulsive signal, and the fixed points of time reassignment operator are equivalent to ridge points of WT, where ridge is the most relevant to the TF features of signals. Therefore, for more general signals, the relationship among the fixed points of the time reassignment operator, ridge points of the WT and GD of signals is particularly important. In this paper, we discuss the relationship among these three, and develop a new GD estimator for strongly frequency-varying signal, which can precisely describe the ridge of WT and accurately estimate the GD of signal. Further we introduce a new frequency-varying TFA method and develop the rigorous theoretical analysis. The main innovations of this paper are:

i) We convert the GD estimation problem into solving the fixed point problem and propose a new GD estimator. We firstly develop a strict equivalence condition between the fixed points of the time reassignment operator and ridge points of WT, and further discuss the relationship among the fixed points of the time reassignment operator, ridge points of the WT and GD of a frequency-varying linear chirp signal. Then, combining these relations with Newton algorithm, we propose a Newton GD estimator, which not only accurately estimates the GD of the signal, but also accurately describes the ridge of WT.

ii) Based on the proposed Newton GD estimator, we propose a Newton time-extracting wavelet transform (NTEWT), which can generate a highly concentrated TFR and reconstruct signal. The main idea of NTEWT is to retain the TF information that are most related to the frequency-varying features of the signal and to remove the weakly-related TF coefficients.

iii) We define a class of weakly-separated frequency-varying chirp-like components (WFCC), which relaxes the strict well-separated condition between components to some extent. The function class we define includes possible interference components and is applicable to a wider range of practical signals.

iv) For such function class, we provide a theoretical analysis for NTEWT under a strict mathematical

framework, and prove that the Newton GD estimator indeed successfully estimates the GD and the NTEWT reconstructs the signal with high accuracy.

The remainder of this paper is organized as follows. In section 2, we discuss the relationship among the fixed points of the time reassignment operator, ridge points of the WT and GD of the signal. Then in section 3, we combine these relations and Newton algorithm to propose a Newton GD estimator. And further, we introduce the NTEWT. In section 4, we analyze the performance of the NTEWT theoretically, including a theorem and its proof about the NTEWT for a class of WFCC. Section 5 is devoted to the comparative study of the NTEWT and other TFA methods on simulated and real signals with three quantitative indicators. Finally, conclusions are drawn in section 6.

2. Time reassignment operator

In this section, we first recall several basic definitions, then study the relationship among the fixed points of the time reassignment operator, ridge points of the WT and GD of the signal.

2.1. Basic Notations and Definitions

Definition 1. [8] *The Fourier transform (FT) of a given signal $x(t) \in L^1(\mathbb{R})$, i.e. its correlation with a sinusoidal wave $e^{i\omega t}$, is defined as:*

$$X(\omega) = \int_{\mathbb{R}} x(t) e^{-i\omega t} dt, \quad (1)$$

and its inverse FT is defined by [8]:

$$x(t) = \frac{1}{2\pi} \int_{\mathbb{R}} X(\omega) e^{i\omega t} d\omega. \quad (2)$$

Definition 2. [41] *The frequency-varying signal is defined in the frequency domain*

$$X(\omega) = A(\omega) e^{-i\phi(\omega)}, \quad (3)$$

where $A(\omega)$ is the signal amplitude, $\phi(\omega)$ and its derivative $\phi'(\omega)$ are the phase and the GD, respectively.

Definition 3. [8] *Consider an admissible wavelet $\psi(t) \in L^2(\mathbb{R})$, its FT satisfies $C_\psi = \int_{\mathbb{R}^+} \frac{|\hat{\psi}(\omega)|^2}{\omega} d\omega < +\infty$, and then the WT of a signal $x(t) \in L^2(\mathbb{R})$ is defined as a complex-valued function of time b and scale $a > 0$ by*

$$W_x^\psi(b, a) = \frac{1}{a} \int_{\mathbb{R}} x(t) \psi^*\left(\frac{t-b}{a}\right) dt, \quad (4)$$

where z^* is the complex conjugate of z . And $W_x^\psi(b, a)$ can be expressed in the frequency domain by Plancherel's theorem

$$W_X^{\hat{\psi}}(b, a) = \frac{1}{2\pi} \int_{\mathbb{R}} X(\omega) \hat{\psi}^*(a\omega) e^{i\omega b} d\omega. \quad (5)$$

where $X(\omega)$ and $\hat{\psi}(\omega)$ are FTs of $x(t)$ and $\psi(t)$, respectively.

Denote $W_X^{\hat{\psi}}(b, a) = M_X^{\hat{\psi}}(b, a) e^{i\Phi_X^{\hat{\psi}}(b, a)}$, $M_X^{\hat{\psi}}(b, a)$ and $\Phi_X^{\hat{\psi}}(b, a)$ stand for magnitude and phase of WT, respectively.

Definition 4. [44] A ridge point of WT $W_X^{\hat{\psi}}(b, a)$ is a time-scale pair (b, a) satisfying the two conditions:

$$\partial_b \ln M_X^{\hat{\psi}}(b, a) = 0, \quad \frac{\partial^2}{\partial b^2} \ln M_X^{\hat{\psi}}(b, a) < 0. \quad (6)$$

where $\partial_b, \frac{\partial^2}{\partial b^2}$ are the first and second order partial derivatives with respect to b , respectively. These conditions state that for each fixed scale a , a time ridge point b corresponds to the time at which a local maximum of magnitude $M_X^{\hat{\psi}}(b, a)$ occurs.

Definition 5. [15] The complex time reassignment operator $\tilde{t}_x(b, a)$ and the time reassignment operator $\hat{t}_x(b, a)$ can be defined respectively by

$$\begin{cases} \tilde{t}_x(b, a) = b + a \frac{W_x^{t\psi}(b, a)}{W_x^{\psi}(b, a)} \\ \hat{t}_x(b, a) = b + a \Re\left\{ \frac{W_x^{t\psi}(b, a)}{W_x^{\psi}(b, a)} \right\}, \end{cases} \quad (7)$$

where $W_x^{\psi}(b, a) \neq 0$ and $\Re\{z\}$ denotes the real part of z .

Definition 6. [45] Metric space (Λ, ρ) is a set Λ together with a metric ρ on the set Λ , we say that a mapping F on (Λ, ρ) is a contraction mapping from Λ to Λ if there exists a constant k such that $0 < k < 1$ and

$$\rho(F(x), F(y)) \leq k\rho(x, y), \quad \forall x, y \in \Lambda. \quad (8)$$

2.2. Time reassignment operator and ridge

In this subsection, we discuss the relationship between the fixed points of the time reassignment operator and ridge points of WT for frequency-varying signals, and we further provide the equivalent conditions between the fixed points and ridge points.

Theorem 1. For any signal $X(\omega) = A(\omega)e^{-i\phi(\omega)}$, consider a Morlet wavelet expressed by

$$\hat{\psi}(\omega) = (4\pi\sigma^2)^{\frac{1}{4}} e^{-\frac{\sigma^2(\omega - \omega_\psi)^2}{2}}, \quad (9)$$

then for any $(b, a) \in \mathbb{R} \times \mathbb{R}^+$, the following statements hold:

(a) $\hat{t}_X(b, a) = b$ if and only if $\partial_b \ln M_X^{\hat{\psi}}(b, a) = 0$.

(b) If $\hat{t}_X(b, a)$ is a contraction operator for a given scale a , then $\hat{t}_X(b, a) = b$ if and only if the point (b, a) is a ridge point.

Proof. (a) For $\hat{\psi}(\omega)$, since $t\psi(t) \xrightarrow{FT} i\hat{\psi}'$ and its derivative $\hat{\psi}'(\omega) = -\sigma^2(\omega - \omega_\psi)\hat{\psi}(\omega)$, it is easy to derive that by Eq. (7)

$$\hat{t}_X(b, a) = b + a \Im\left\{ \frac{W_X^{\hat{\psi}'}(b, a)}{W_X^{\hat{\psi}}(b, a)} \right\} = b - a\sigma^2 \Im\left\{ \frac{W_X^{\omega\hat{\psi}}(b, a)}{W_X^{\hat{\psi}}(b, a)} \right\}, \quad (10)$$

where $\Im\{z\}$ is the imaginary part of z . On the other hand, noting that $\partial_b W_X^{\omega\hat{\psi}}(b, a) = \frac{i}{a} W_X^{\omega\hat{\psi}}(b, a)$, it follows that

$$\Re\{\partial_b \ln W_X^{\hat{\psi}}(b, a)\} = -\Im\left\{ \frac{W_X^{\omega\hat{\psi}}(b, a)}{a W_X^{\hat{\psi}}(b, a)} \right\}. \quad (11)$$

According to Eqs. (10) and (11), and noticing that $\partial_b \ln M_X^{\hat{\psi}}(b, a) = \Re\{\partial_b \ln W_X^{\hat{\psi}}(b, a)\}$, we get

$$\hat{t}_X(b, a) = b + a^2 \sigma^2 \partial_b \ln M_X^{\hat{\psi}}(b, a). \quad (12)$$

Then, Theorem 1 (a) holds.

(b) Assume b^* is a fixed point of $\hat{t}_X(b, a)$, i.e. $\hat{t}_X(b^*, a) = b^*$. Then, for proving that (b^*, a) is a ridge point, we only need to show $\frac{\partial^2}{\partial b^2} \ln M_X^{\hat{\psi}}(b^*, a) < 0$, by Eq. (12) which is equivalent to prove $\partial_b \hat{t}_X(b^*, a) < 1$. Consider a sequence $\{b_n\}_{n=1}^{+\infty}$ with $\lim_{n \rightarrow +\infty} b_n = b^*$, and denote $F(b) = \hat{t}_X(b, a)$. Since $\hat{t}_X(b, a)$ is a contraction operator, by Definition 6, there exists a constant k such that $0 < k < 1$ and

$$|F(b_{n+1}) - F(b_n)| \leq k \cdot |b_{n+1} - b_n|, \quad n = 1, 2, \dots \quad (13)$$

Thanks to the regularity of the WT, the function $F(b)$ is continuously differentiable, then this follows that there exists a ξ_n being between b_n and b_{n+1} , such that

$$|F'(\xi_n)| \leq k, \quad n = 1, 2, \dots \quad (14)$$

Due to $\lim_{n \rightarrow +\infty} b_n = b^*$, it deduces that $|F'(b^*)| \leq k$, that is $|\partial_b \hat{t}_X(b^*, a)| \leq k < 1$. Assume (b, a) is a ridge point, then by (a), we have $\hat{t}_X(b, a) = b$. Hence, Theorem 1 (b) holds.

Theorem 1 well reveals the existence of the fixed points of the time reassignment operator, explains the relationship between the fixed points of the time reassignment operator and ridge points of WT, and provides equivalent condition of the two, i.e. $\hat{t}_x(b, a)$ is a contraction operator. Since the fixed points of the contraction operator exist and are unique, the ridge points exist and are unique. In the next subsection, we will use a frequency-varying linear chirp signal to verify Theorem 1.

2.3. Time reassignment operator and GD

For a frequency-varying linear chirp signal $X(\omega)$, the following lemma shows that $\hat{t}_X(b, a)$ is a contraction operator and further gives the relations among the fixed points of $\hat{t}_X(b, a)$, ridge points of WT and GD of $X(\omega)$.

Lemma 1. For a frequency-varying linear chirp signal,

$$X(\omega) = A e^{-i\phi(\omega)}, \quad (15)$$

where $\phi(\omega) = \frac{\alpha}{2}\omega^2 + \beta\omega + \gamma$, consider the Morlet wavelet $\hat{\psi}(\omega) = (4\pi\sigma^2)^{\frac{1}{4}} e^{-\frac{\sigma^2(\omega - \omega_{\psi})^2}{2}}$. Then, for any given scale $a > 0$, the following hold:

- (a) $\hat{t}_X(b, a)$ is a contraction operator.
- (b) $\hat{t}_X(b, a)$ is a biased estimate of the signal GD.
- (c) $\hat{t}_X(b, a) = b$ if and only if the point (b, a) is at the GD trajectory of signal $X(\omega)$.
- (d) $\hat{t}_X(b, a) = b$ if and only if the point (b, a) is a ridge point of WT $W_X^{\hat{\psi}}(b, a)$.

Proof. (a) Since ω_ψ is the frequency center of the Morlet wavelet $\hat{\psi}(\omega)$, the frequency ω and scale a are related by

$$\omega = \frac{\omega_\psi}{a}. \quad (16)$$

Thus, the GD of signal $X(\omega)$ can be expressed as

$$\phi'(\frac{\omega_\psi}{a}) = \alpha \frac{\omega_\psi}{a} + \beta. \quad (17)$$

A straightforward computation shows that the WT $W_X^{\hat{\psi}}(b, a)$ and $W_X^{\hat{\psi}'}(b, a)$ of $X(\omega)$ can be expressed as

$$\begin{aligned} W_X^{\hat{\psi}}(b, a) &= Ae^{-i(\frac{\alpha}{2})(\frac{\omega_\psi}{a})^2 + \beta \frac{\omega_\psi}{a} + \gamma} e^{i \frac{\omega_\psi}{a} b} \sqrt{\frac{\sigma(a^2\sigma^2 - i\alpha)}{\pi^{\frac{1}{2}}(a^4\sigma^4 + \alpha^2)}} e^{-\frac{a^2(a^2\sigma^2 - i\alpha)}{2(a^4\sigma^4 + \alpha^2)} (\frac{\alpha \frac{\omega_\psi}{a} + \beta - b)^2} \\ &= \frac{1}{a} X(\frac{\omega_\psi}{a}) C_x(b, a), \\ W_X^{\hat{\psi}'}(b, a) &= \frac{i\sigma^2(a^2\sigma^2 - i\alpha)}{a^4\sigma^4 + \alpha^2} (\alpha \frac{\omega_\psi}{a} + \beta - b) e^{i \frac{\omega_\psi}{a} b} X(\frac{\omega_\psi}{a}) C_x(b, a), \end{aligned} \quad (18)$$

where $C_x(b, a) = \sqrt{\frac{a^2\sigma(a^2\sigma^2 - i\alpha)}{\pi^{\frac{1}{2}}(a^4\sigma^4 + \alpha^2)}} e^{-\frac{a^2(a^2\sigma^2 - i\alpha)}{2(a^4\sigma^4 + \alpha^2)} (\frac{\alpha \frac{\omega_\psi}{a} + \beta - b)^2}$.

Therefore, by the definition of complex time reassignment operator $\tilde{t}_X(b, a)$ in Eq. (7) and Eq. (18), we have

$$\tilde{t}_X(b, a) = b - ia \frac{W_X^{\hat{\psi}'}(b, a)}{W_X^{\hat{\psi}}(b, a)} = b - \frac{a^2\sigma^2(a^2\sigma^2 - i\alpha)}{a^4\sigma^4 + \alpha^2} (b - \alpha \frac{\omega_\psi}{a} - \beta). \quad (19)$$

It follows that the time reassignment operator $\hat{t}_X(b, a) = \Re\{\tilde{t}_X(b, a)\}$ can be expressed as

$$\hat{t}_X(b, a) = b - \frac{a^4\sigma^4}{a^4\sigma^4 + \alpha^2} (b - \alpha \frac{\omega_\psi}{a} - \beta) = \frac{\alpha^2 b + a^4\sigma^4(\alpha \frac{\omega_\psi}{a} + \beta)}{a^4\sigma^4 + \alpha^2}. \quad (20)$$

Thus, for any given a , we have

$$0 \leq \partial_b \hat{t}_X(b, a) = \frac{\alpha^2}{a^4\sigma^4 + \alpha^2} < 1, \quad (21)$$

that is, $\hat{t}_X(b, a)$ is a contraction operator.

(b) For any given scale a , Eqs. (17) and (20) shows that $\hat{t}_X(b, a)$ is a biased GD estimator.

(c) According to Eq. (20), the fixed point curve of $\hat{t}_X(b, a)$ can be expressed as

$$b = \alpha \frac{\omega_\psi}{a} + \beta, \quad a > 0. \quad (22)$$

Hence, by Eq. (22) and the GD expression of signal $X(\omega)$ in Eq. (17), one can get immediately that Lemma 1 (c) holds.

(d) The derivative of $\ln W_X^{\hat{\psi}}(b, a)$ with respect to time b is calculated as

$$\partial_b \ln W_X^{\hat{\psi}}(b, a) = i \frac{\omega_\psi}{a} - \frac{a^2\sigma^2 - i\alpha}{a^4\sigma^4 + \alpha^2} (b - \alpha \frac{\omega_\psi}{a} - \beta). \quad (23)$$

This, together with the fact $\partial_b \ln M_X^{\hat{\psi}}(b, a) = \Re\{\partial_b \ln W_X^{\hat{\psi}}(b, a)\}$, implies

$$\partial_b \ln M_X^{\hat{\psi}}(b, a) = -\frac{a^2\sigma^2}{a^4\sigma^4 + \alpha^2} (b - \alpha \frac{\omega_\psi}{a} - \beta), \quad (24)$$

and

$$\frac{\partial^2}{\partial b^2} \ln M_X^{\hat{\psi}}(b, a) < 0. \quad (25)$$

Thus, the ridge trajectory of WT $W_X^{\hat{\psi}}(b, a)$ can be written as

$$b = \alpha \frac{\omega_\psi}{a} + \beta, \quad a > 0. \quad (26)$$

This, together with Eq. (22), lead to the conclusion that Lemma 1 (d) holds.

It can be concluded from Lemma 1 that for the frequency-varying linear chirp signal $X(\omega)$: (1) $\hat{t}_X(b, a)$ is a biased estimate of the GD of $X(\omega)$; (2) the fixed point of time reassignment operator $\hat{t}_X(b, a)$ is an accurate estimate of the GD; (3) the GD trajectory of signal $X(\omega)$ and the ridge trajectory of WT $W_X^{\hat{\psi}}(b, a)$ are the same.

3. Newton time-extracting wavelet transform

3.1. Newton group delay estimator

As can be seen from the previous section, for the frequency-varying linear chirp signal $X(\omega)$, the time reassignment operator $\hat{t}_X(b, a)$ can't estimate the GD of $X(\omega)$ accurately, but the fixed points of the time reassignment operator can. Indeed, the fixed points of the time reassignment operator can not only accurately estimate the GD of the signal, but also precisely describe the ridge of WT. Therefore, the GD estimation problem is converted into the problem for solving the fixed points of the time reassignment operator, then we can try to employ some root finding algorithms to derive a new GD estimator. Inspired by the relations between Eqs. (17), (19) and (22), we use Newton algorithm to estimate GD in the following.

Lemma 2. For a frequency-varying linear chirp signal,

$$X(\omega) = Ae^{-i\phi(\omega)}, \quad (27)$$

where $\phi(\omega) = \frac{\alpha}{2}\omega^2 + \beta\omega + \gamma$, consider the Morlet wavelet $\hat{\psi}(\omega) = (4\pi\sigma^2)^{\frac{1}{4}}e^{-\frac{\sigma^2(\omega-\omega_\psi)^2}{2}}$. Let

$$\bar{t}_X(b, a) = b - \frac{b - \tilde{t}_X(b, a)}{1 - \partial_b \tilde{t}_X(b, a)}. \quad (28)$$

Then the following hold:

- (a) $\bar{t}_X(b, a) = b$ if and only if $\tilde{t}_X(b, a) = b$.
- (b) $\bar{t}_X(b, a)$ is an accurate GD estimation of the signal $X(\omega)$.
- (c) $\bar{t}_X(b, a) = b$ if and only if the point (b, a) is at the GD trajectory of signal $X(\omega)$.
- (d) $\bar{t}_X(b, a) = b$ if and only if the point (b, a) is a ridge point of WT $W_X^{\hat{\psi}}(b, a)$.

Proof. (a) By Eq. (19), we immediately get

$$\partial_b \tilde{t}_X(b, a) = 1 - \frac{a^2\sigma^2(a^2\sigma^2 - i\alpha)}{a^4\sigma^4 + \alpha^2}, \quad (29)$$

it means that we have $1 - \partial_b \tilde{t}_X(b, a) \neq 0$. Thus, by Eq. (28), $\bar{t}_X(b, a) = b$ if and only if $\tilde{t}_X(b, a) = b$.

(b) Combining Eq. (19) with Eq. (29), we have

$$\tilde{t}_X(b, a) = b - (1 - \partial_b \tilde{t}_X(b, a))(b - \alpha \frac{\omega_\psi}{a} - \beta).$$

Thus, for any $(b, a) \in \mathbb{R} \times \mathbb{R}^+$, we have

$$\bar{t}_X(b, a) = b - \frac{b - \tilde{t}_X(b, a)}{1 - \partial_b \tilde{t}_X(b, a)} = \alpha \frac{\omega_\psi}{a} + \beta = \phi'(\frac{\omega_\psi}{a}). \quad (30)$$

that is, $\bar{t}_X(b, a)$ is an accurate GD estimation of the signal $X(\omega)$.

(c) According to Eq. (30), one has $\bar{t}_X(b, a) = b$ if and only if the point (b, a) is at the GD trajectory of signal $X(\omega)$, i.e.

$$b = \alpha \frac{\omega_\psi}{a} + \beta. \quad (31)$$

(d) Combining Eq. (26) with Eq. (30), we have $\bar{t}_X(b, a) = b$ if and only if the point (b, a) is a ridge point of WT.

Eq. (28) can be considered as the first iteration of the Newton algorithm for solving the fixed point equation $\tilde{t}_X(s, a) = s$, in which a sequence defined in the scalar case as $s_{n+1} = s_n - \frac{f(s_n)}{f'(s_n)}$, is hoped to converge to a root of the equation $f(s) = 0$, where $f(s) = s - \tilde{t}_X(s, a)$, with $s_0 = b$. Thus, we have the following definition:

Definition 7. A Newton GD (NGD) estimator $\bar{t}_X(b, a)$ can be defined by

$$\bar{t}_X(b, a) = b - \frac{b - \tilde{t}_X(b, a)}{1 - \partial_b \tilde{t}_X(b, a)}. \quad (32)$$

It is noteworthy that we convert GD estimation problem into solving the fixed point problem, and propose the NGD estimator $\bar{t}_X(b, a)$ combined with Newton algorithm. It is a new attempt to estimate GD, which also allows to design other GD estimators from other root finding algorithms.

It can be found that various IF estimators, presented in [7], [23], [27], [28], [32], [34], are usually suitable for estimating the IF of slowly or strongly time-varying signals, but they aren't suitable for impulsive signals whose TF ridge curves are nearly perpendicular to the time axis. For analyzing impulsive signals, GD estimation is often more appropriate than IF estimation. The proposed NGD estimator can not only accurately estimate the GD of impulsive signals, but also further estimate the GD of second-order frequency-varying signals. Especially for frequency-varying linear chirp signal $X(\omega)$, NGD estimator can accurately estimate the GD of $X(\omega)$ and describe the ridge of WT.

From the comparison between those IF estimators and NGD estimator, we found that those IF estimators perform better for estimating the IF of slowly or strongly time-varying signals, while NGD estimator can accurately estimate the GD of slowly or strongly frequency-varying signals. Therefore, NGD estimator and those IF estimators are complementary with each other and each of them has respective scope of application.

3.2. NTEWT

In this subsection, we extend TEWT to the second-order case based on the Newton GD estimator, and propose a new TFA post-processing method extracting along the time direction.

Definition 8. *The Newton time-extracting wavelet transform (NTEWT) is defined as*

$$NTe(b, a) = W_X^{\psi}(b, a) \cdot \delta(b - \bar{t}_X(b, a)). \quad (33)$$

It is well known that SWT [23] is designed for local harmonic signal in the time domain, MSWT [7] is designed for local constant amplitude-modulated linear chirp signal in the time domain, and SMEWT [34] is designed for local Gaussian amplitude-modulated linear chirp in the time domain. Thus, these TFA methods reassigning or extracting along the frequency direction are suitable for dealing with slowly or strongly varying signals in the time domain. However, the TSST [36], TSWT [38] and TEWT [39] are suitable for impulsive-like signals, and the proposed NTEWT is designed for frequency-varying linear chirp signal. Therefore, these TFA methods reassigning or extracting along the time direction are suitable for characterizing slowly or strongly varying signals in the frequency domain.

Differing from the squeezing manner of synchrosqueezing methods [7], [23], [27], [36], [38], [40], the NTEWT only extracts the WT coefficients at the fixed point trajectory $b = \bar{t}_X(b, a)$, while removing the TF coefficients beyond the fixed point trajectory $b = \bar{t}_X(b, a)$. In particular, for the frequency-varying linear chirp signal $X(\omega)$, it can be concluded from the above discussion that: (1) by Lemma 2 (c), the NTEWT exactly extracts the WT coefficients at the GD trajectory of signal; (2) as shown in Lemma 2 (d), the fixed points of the NGD estimator $\bar{t}_X(b, a)$ are the time ridge points, which means that NTEWT can remain the maximum energy of the WT modulus, then NTEWT can obtain a more energy concentrated TFR; (3) According to Eq. (18), NTEWT maintains the reconstructed property of WT, and signal $X(\omega)$ can be recovered by WT along the GD trajectory, i.e.,

$$X\left(\frac{\omega_\psi}{a}\right) = \frac{aW_x^{\psi}\left(\phi'\left(\frac{\omega_\psi}{a}\right), a\right)e^{-i\frac{\omega_\psi}{a}b}}{C_x\left(\phi'\left(\frac{\omega_\psi}{a}\right), a\right)}. \quad (34)$$

It motivates us to recover signal $X(\omega)$ from the NTEWT with a similar reconstruction expression:

$$X\left(\frac{\omega_\psi}{a}\right) = \frac{aNTe\left(\phi'\left(\frac{\omega_\psi}{a}\right), a\right)e^{-i\frac{\omega_\psi}{a}b}}{C_x\left(\phi'\left(\frac{\omega_\psi}{a}\right), a\right)}. \quad (35)$$

4. Theoretical analysis of Newton time-extracting wavelet transform

In this section, we will provide a rigorous theoretical analysis of NTEWT that can identify and characterize a function class $\mathcal{C}_{\epsilon, d}$. To better understand the function class $\mathcal{C}_{\epsilon, d}$ for NTEWT, let's first review a function class $\mathcal{H}_{\epsilon, d}$ for TSWT.

Definition 9. [38] *The class $\mathcal{H}_{\epsilon, d}$ is said to be a set of all superposition of well-separated frequency-domain harmonic-like functions, with accuracy $\epsilon > 0$ and separation $d > 0$, if each element $X(\omega) =$*

$\sum_{k=1}^K X_k(\omega) = \sum_{k=1}^K A_k(\omega) e^{-i\phi_k(\omega)} \in L^\infty(\mathbb{R})$, with $A_k(\omega) \in C^1(\mathbb{R}) \cap L^\infty(\mathbb{R})$ and $\phi_k(\omega) \in C^2(\mathbb{R})$ satisfying:

$$\begin{aligned} m_k &= \sup_{\omega \in \mathbb{R}^+} |A_k(\omega)|, \quad m'_k = \sup_{\omega \in \mathbb{R}^+} |\phi'_k(\omega)|, \quad |A'_k(\omega)|, \quad |\phi''_k(\omega)| \leq \epsilon |\phi'_k(\omega)|, \quad \forall \omega \in \mathbb{R}^+, \\ \phi'_{k+1}(\omega) - \phi'_k(\omega) &\geq \frac{d}{\omega}, \quad \forall \omega \in \mathbb{R}^+, \quad k \in \{1, 2, \dots, K-1\}. \end{aligned} \quad (36)$$

Intuitively, for the function class $\mathcal{H}_{\epsilon,d}$, each component $X_k(\omega)$ can be viewed as approximately a harmonic signal locally in the frequency domain, with slowly varying amplitude $A_k(\omega)$ and GD $\phi'_k(\omega)$. In Theorem 3.1 for the TSWT [38], it has been shown that $X_k(\omega)$ and $X_{k+1}(\omega)$ satisfying well-separated conditions ($\phi'_{k+1}(\omega) - \phi'_k(\omega) \geq \frac{d}{\omega}$ with $d > 2\omega_\psi \Delta$) are separated. It has been also proven that the energy of WT $W_{X_k}^{\hat{\psi}}(b, a)$ of the k th component $X_k(\omega)$ is concentrated in the zone $Z_k := \{(b, a); |\frac{\phi'_k(\frac{\omega_\psi}{a}) - b}{a}| < \Delta\}$, and the energy distribution of $W_X^{\hat{\psi}}(b, a)$ is concentrated in the zones $\bigcup_{1 \leq k \leq K} Z_k$. Thus, zone Z_k provides an estimate of the main energy distribution region of $W_X^{\hat{\psi}}(b, a)$. Compared with the class $\mathcal{H}_{\epsilon,d}$ for TSWT, the class $\mathcal{C}_{\epsilon,d}$ for NTEWT is not restricted to the class $\mathcal{H}_{\epsilon,d}$ composed of several harmonic-like components, which is mathematically defined as:

Definition 10. *The class $\mathcal{C}_{\epsilon,d}$ is said to be a set of all superposition of weakly-separated frequency-varying chirp-like components (WFCC) up to accuracy $\epsilon > 0$ and with separation $d_{k,k+1} > 0$, if each element $X(\omega) = \sum_{k=1}^K X_k(\omega) = \sum_{k=1}^K A_k(\omega) e^{-i\phi_k(\omega)}$ satisfies the following four conditions:*

(1) *Regularity conditions:*

$$A_k(\omega) \in L^\infty(\mathbb{R}) \cap C^2(\mathbb{R}), \quad \phi_k(\omega) \in C^3(\mathbb{R}), \quad k \in \{1, 2, \dots, K\}.$$

(2) *Boundedness conditions:*

$$0 < \inf_{\omega \in \mathbb{R}} A_k(\omega) \leq \sup_{\omega \in \mathbb{R}} A_k(\omega) < +\infty, \quad k \in \{1, 2, \dots, K\}$$

$$0 < \inf_{\omega \in \mathbb{R}} \phi'_k(\omega) \leq \sup_{\omega \in \mathbb{R}} \phi'_k(\omega) < +\infty, \quad \sup_{\omega \in \mathbb{R}} |\phi''_k(\omega)| < +\infty.$$

(3) *Growth conditions:*

$$|A'_k(\omega)|, \quad |\phi'''_k(\omega)| \leq \epsilon |\phi''_k(\omega)|, \quad k \in \{1, 2, \dots, K\}.$$

(4) *Weakly-separated conditions: $X_k(\omega)$ are separated with the distance $d_{k,k+1} > 0$, i.e.*

$$\phi'_{k+1}(\omega) - \phi'_k(\omega) \geq \frac{d_{k,k+1}}{\omega}, \quad \omega \in \mathbb{R}^+, \quad k \in \{1, 2, \dots, K-1\}. \quad (37)$$

Intuitively, the function class $\mathcal{C}_{\epsilon,d}$ is composed of several oscillatory components $X_k(\omega)$, where the change rate (in frequency) of $A_k(\omega)$ and $\phi'_k(\omega)$ is much smaller than the change rate of $\phi'_k(\omega)$ itself, which means that each component $X_k(\omega)$ can be viewed as approximately a chirp signal locally in the frequency domain, with slowly varying amplitude $A_k(\omega)$ and $\phi''_k(\omega)$. It is worth noting that, different from the constant separation constant d in the well-separated condition (36), each separation constant $d_{k,k+1}$ in the weakly-separated condition (37) here varies with components.

Our main result is then the following:

Theorem 2. Let $X(\omega) = \sum_{k=1}^K X_k(\omega) \in \mathcal{C}_{\epsilon,d}$, and set $\tilde{\epsilon} := \epsilon^{\frac{1}{4}}$. Pick a wavelet $\hat{\psi}(\omega)$ such that inverse FT $\psi_\phi(t)$ of its variant $\hat{\psi}_\phi(\omega) = e^{i\phi_k''(\frac{\omega_\psi}{a})\frac{\omega^2}{2a^2}} \hat{\psi}(\omega + \omega_\psi)$ satisfies the following conditions: if $|t| > \Delta_k$ with $d_{k,k+1} > \max\{\omega_\psi \Delta_k, \omega_\psi \Delta_{k+1}\}$, $\psi_\phi(t) \leq \epsilon G_0$, $\psi'_\phi(t) \leq \epsilon G_1$, $\psi''_\phi(t) \leq \epsilon G_2$, with G_0, G_1, G_2 being some constants. Consider the WT $W_X^{\hat{\psi}}(b, a)$ of $X(\omega)$ with respect to $\hat{\psi}(\omega)$, as well as the NTEWT $NTe(b, a)$. For $k \in \{1, 2, \dots, K-1\}$, define a set $T_k := \{(b, a); \Pi_k(a) < b < \Pi^k(a)\}$, with

$$\begin{aligned} \Pi_k(a) &= \max\{\phi'_{k-1}(\frac{\omega_\psi}{a}) + a\Delta_{k-1}, \phi'_k(\frac{\omega_\psi}{a}) - a\Delta_k\}, \quad \Pi_1(a) = \phi'_1(\frac{\omega_\psi}{a}) - \Delta_1, \\ \Pi^k(a) &= \min\{\phi'_k(\frac{\omega_\psi}{a}) + a\Delta_k, \phi'_{k+1}(\frac{\omega_\psi}{a}) - a\Delta_{k+1}\}, \quad \Pi^K(a) = \phi'_K(\frac{\omega_\psi}{a}) + \Delta_K, \end{aligned} \quad (38)$$

Then, provided ϵ is sufficiently small, the following hold:

(a) For $k \in \{1, 2, \dots, K-1\}$, and for each pair (b, a) , we have $T_k \neq \emptyset$ with $(\phi'_k(\frac{\omega_\psi}{a}), a) \in T_k$, and $T_k \cap T_{k+1} = \emptyset$.

(b) For each $k \in \{1, \dots, K-1\}$, and for each pair $(b, a) \in T_k$ for which holds $|W_X^{\hat{\psi}}(b, a)| > \tilde{\epsilon}$, then we have

$$|\bar{t}_X(b, a) - \phi'_k(\frac{\omega_\psi}{a})| \leq \tilde{\epsilon}. \quad (39)$$

(c) Moreover, for each $k \in \{1, \dots, K\}$, and for each pair $(b, a) \in T_k$, there exists a constant $C > 0$ such that,

$$\left| \frac{2\pi a NTe(\phi'_k(\frac{\omega_\psi}{a}), a) e^{-i\frac{\omega_\psi}{a}\phi'_k(\frac{\omega_\psi}{a})}}{\psi_\phi^*(0)} - X_k(\frac{\omega_\psi}{a}) \right| \leq C\tilde{\epsilon}.$$

Theorem 2 basically tells us that:

(a) If $d_{k,k+1} > \max\{\omega_\psi \Delta_k, \omega_\psi \Delta_{k+1}\}$, then weakly-separated chirp-like components of $\mathcal{C}_{\epsilon,d}$ may interfere with each other. However, each zone T_k does not intersect with each other, the zone T_k corresponds to the energy distribution region of $W_X^{\hat{\psi}}(b, a)$ of the k th component $X_k(\omega)$ at the point $(\phi'_k(\frac{\omega_\psi}{a}), a)$ and its vicinity, and the zone T_k for component $X_k(\omega)$ is separated from the main energy distribution regions of WT of other components.

(b) The NGD estimator $\bar{t}_X(b, a)$ is indeed a high-precision GD estimator in the zone T_k .

(c) The signal can be reconstructed with reasonably high accuracy by NTEWT.

The proof of this theorem is available in Appendix A. In the Lemma 3 of Appendix A, to further compare T_k and Z_k , we modify the set Z_k for TSWT [38], i.e. $Z_k = \{(b, a); |\frac{\phi'_k(\frac{\omega_\psi}{a}) - b}{a}| < \Delta\}$ and well-separated condition $\phi'_{k+1}(\omega) - \phi'_k(\omega) \geq \frac{d}{\omega}$ with $d > 2\omega_\psi \Delta$. In Lemma 3, we define a set $Z_k := \{(b, a); |\frac{\phi'_k(\frac{\omega_\psi}{a}) - b}{a}| < \Delta_k\}$ and well-separated condition $\phi'_{k+1}(\omega) - \phi'_k(\omega) \geq \frac{d_{k,k+1}}{\omega}$ with $d_{k,k+1} > \omega_\psi (\Delta_k + \Delta_{k+1})$. The set Z_k we define in Lemma 3 is slightly different from the set Z_k for TSWT [38], we assume $d_{k,k+1}$ and Δ_k vary with components, but d and Δ in [38] are constant.

The focus here is on proving that: (1) the relationship between T_k satisfying weakly-separated condition and Z_k satisfying well-separated condition; (2) if the change-rate (in frequency) of the $A_k(\omega)$ and $\phi''_k(\omega)$ is small, compared with the change-rate of the GD $\phi'_k(\omega)$ themselves, then the proposed method

will identify and characterize the information of the signal $X(\omega)$ and their GDs. It can be concluded that, for frequency-varying signals with weakly-separated chirp-like components, the NTEWT can effectively represent them with satisfied TF energy concentration and reasonable reconstruction accuracy. Besides, in the future, we will try to follow the ideas and analysis methods of Daubechies [46] and Sejdić [47] about the theoretical analysis of noise, to further carry out a detailed and in-depth theoretical analysis of noise.

5. Numerical Analysis of the Behavior of NTEWT and Comparisons

In this section, we will compare the difference between the proposed NTEWT method and advanced TFA methods in addressing simulated and real signals, including SWT [23], MSWT [7], RS [15], TSST [36], and TSST2 [41], and we use three quantitative indicators, including the Rényi entropy [7], mean relative error (MRE) [34] and reconstruction quality factor (RQF) [40], to evaluate the TF energy concentration, GD estimation and signal reconstruction performance, respectively.

5.1. Simulation study and performance analysis

The TF concentration is one of the outstanding features used for evaluating the TF performance of TFA methods, which can be quantified by Rényi entropy. The Rényi entropy of α order for TFR is defined as [7]

$$R_\alpha = \frac{1}{1-\alpha} \log_2 \int \int \left(\frac{TFR(b, \omega)}{\int \int TFR(b, \omega) db d\omega} \right)^\alpha db d\omega. \quad (40)$$

where a smaller Rényi entropy value indicates that the TFA method can generate a more energy-concentrated TFR.

Herein, a simulated signal consisting of two components can be constructed in the frequency domain as:

$$X(\omega) = X_1(\omega) + X_2(\omega) = A_1(\omega)e^{-i\phi_1(\omega)} + A_2(\omega)e^{-i\phi_2(\omega)}, \quad (41)$$

where the higher the frequency, the closer the distance between the two components of $X(\omega)$:

$$\begin{aligned} A_1(\omega) &= A_2(\omega) = e^{0.001\omega}, \\ \phi_1(\omega) &= -0.001\omega^3 + 0.16\omega^2 + 1.2\omega, \\ \phi_2(\omega) &= 0.03\omega^2 + 5.2\omega + 250 \ln(0.05\omega + 0.6). \end{aligned} \quad (42)$$

Figs. 1, 2 show the TF results obtained by different TFA methods in addressing frequency-varying signals $X(\omega)$, where third-order Rényi entropy values are displayed in the bottom. It can be observed that some TFA post-processing methods along the frequency direction, such as SWT and MSWT, provide blurred TFRs for frequency-varying signals $X(\omega)$. However, some TFA post-processing methods along the time direction, such as TSST, TSST2 and NTEWT, improve the readability of TFRs of frequency-varying signals $X(\omega)$. The RS along the time and frequency directions also obtain a high resolution TFR. Compared with the other five methods, NTEWT generates the most concentrated TFR, obtains the least

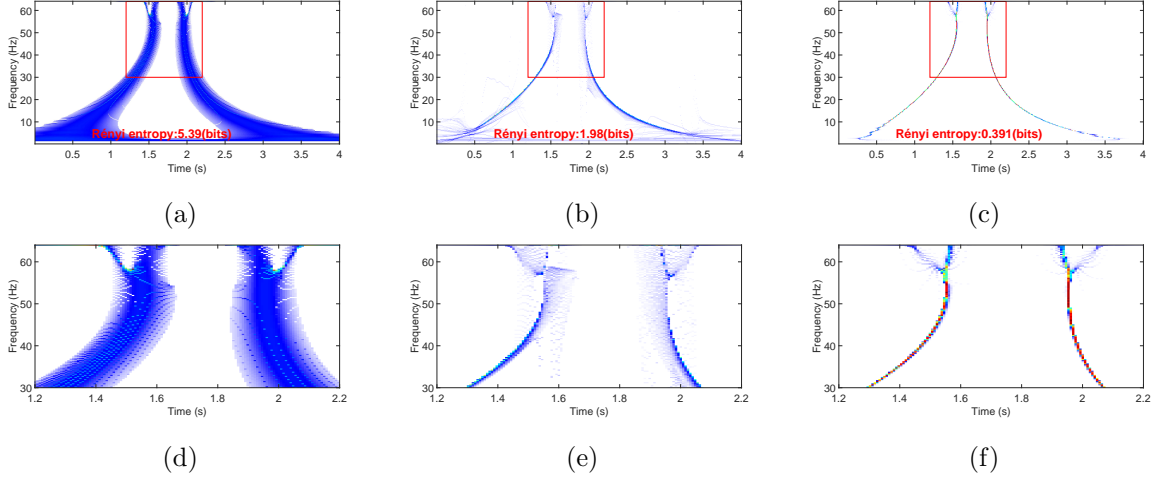


Figure 1: TF results for $X(\omega)$: (a) SWT, (b) MSWT, (c) RS, (d) zoom of the SWT, (e) zoom of the MSWT, (f) zoom of the RS.

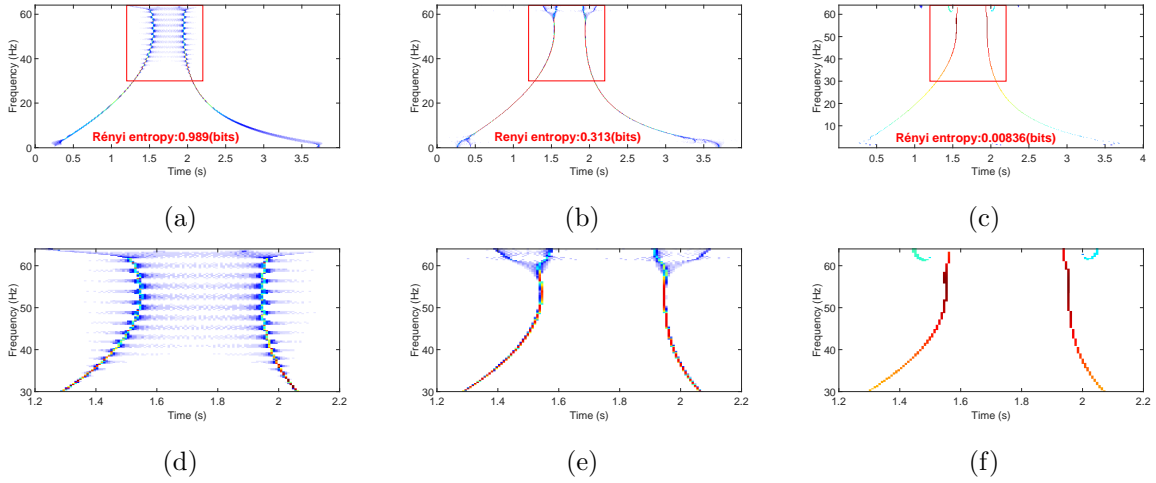


Figure 2: TF results for $X(\omega)$: (a) TSST, (b) TSST2, (c) NTEWT, (d) zoom of the TSST, (e) zoom of the TSST2, (f) zoom of the NTEWT.

Rényi entropy, and suffers the least interference at high frequency, which means the NTEWT behaves the best TF concentration performance for $X(\omega)$. Meanwhile, Table 1 lists the numerical execution time of these TFA methods in addressing frequency-varying signals $X(\omega)$. It can be seen that under the framework of STFT, TSST and TSST2 can finish the analysis within one second. However, these TFA methods under the framework of WT need more time than TSST and TSST2, while NTEWT needs much less time than SWT, MSWT and RS.

In order to study the performance of TF concentration of those TFA methods in the presence of noise, we add Gaussian white noise with signal-to-noise ratio (SNR) of 0 dB to the test signal (see Fig. 3 and Fig. 4). Compared with other TF results, NTEWT achieves the highest resolution TFR and obtains the

Table 1: REQUIRED COMPUTATION TIME.

TFA	SWT	MSWT	RS	TSST	TSST2	NTEWT
Time(s)	4.749	7.928	5.255	0.134	0.211	2.663

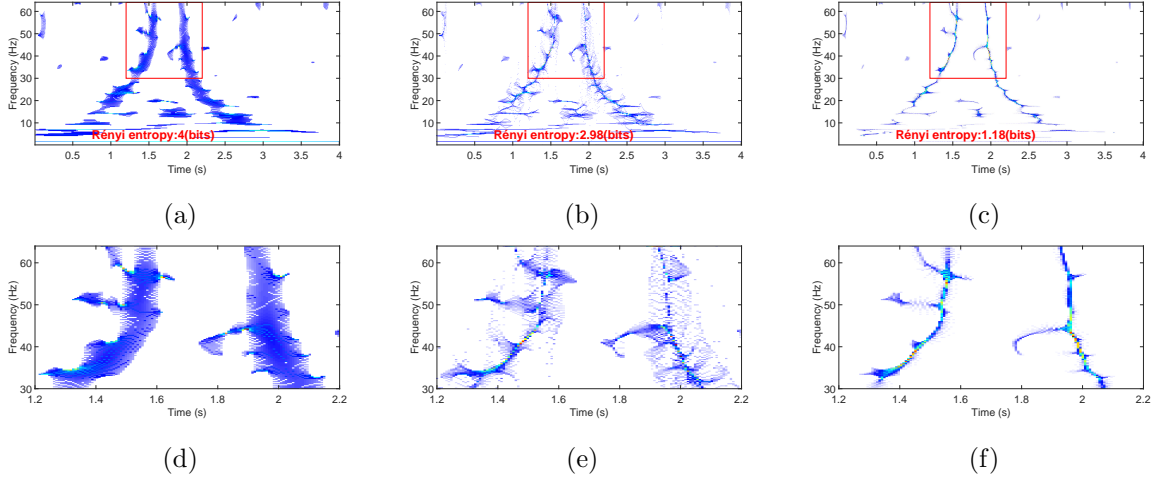


Figure 3: TF results for $X(\omega)$ with SNR=0 dB Gaussian white noise: (a) SWT, (b) MSWT, (c) RS, (d) zoom of the SWT, (e) zoom of the MSWT, (f) zoom of the RS.

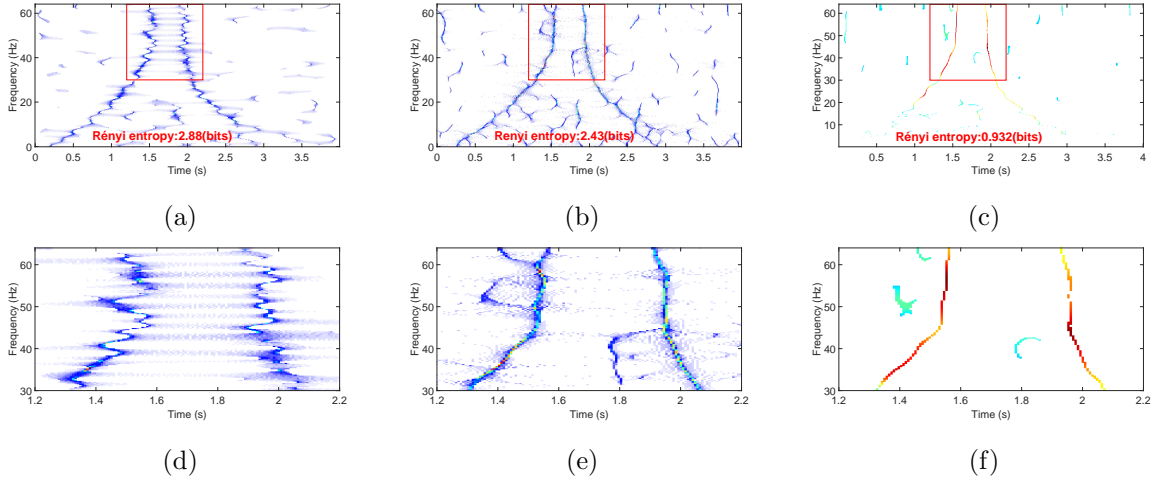


Figure 4: TF results for $X(\omega)$ with SNR=0 dB Gaussian white noise: (a) TSST, (b) TSST2, (c) NTEWT, (d) zoom of the TSST, (e) zoom of the TSST2, (f) zoom of the NTEWT.

least Rényi entropy. Therefore, the NTEWT has clear advantages in addressing strongly-varying signals in the frequency domain, even in noisy conditions.

To further compare the TF concentration performance of these TFA methods under different noise levels, Fig. 5 displays the Rényi entropy curves of five TFA methods under SNRs of 0 dB to 30 dB. It can be shown that, no matter under any SNR, the Rényi entropy curves of NTEWT and RS are always

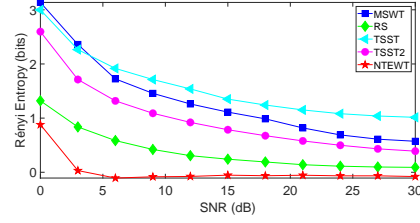


Figure 5: Under different noise levels (SNRs of 0-30 (dB)), Rényi entropy curves of TFRs generated by TFA methods.

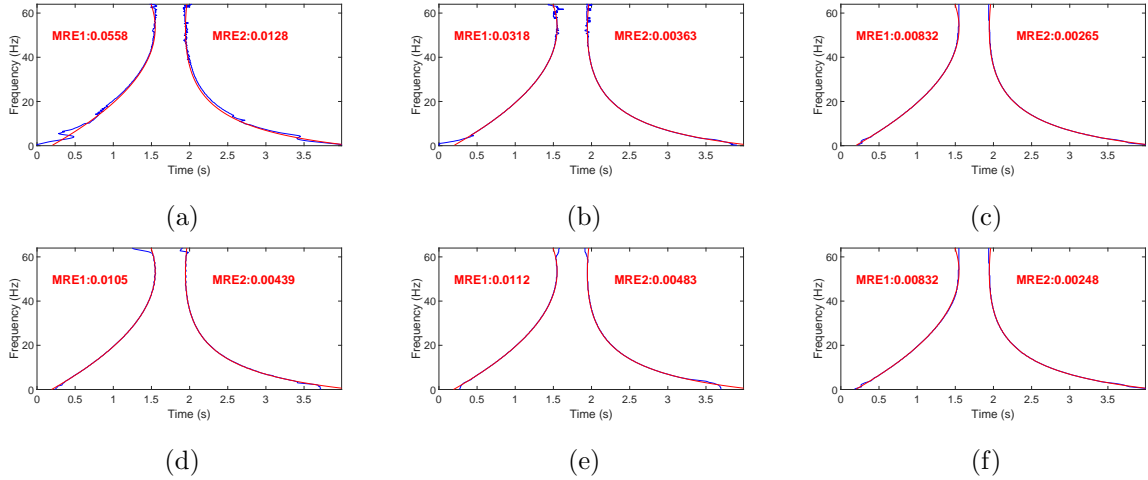


Figure 6: The comparisons of GD estimation: (a) SWT, (b) MSWT, (c) RS, (d) TSST, (e) TSST2, (f) NTEWT.

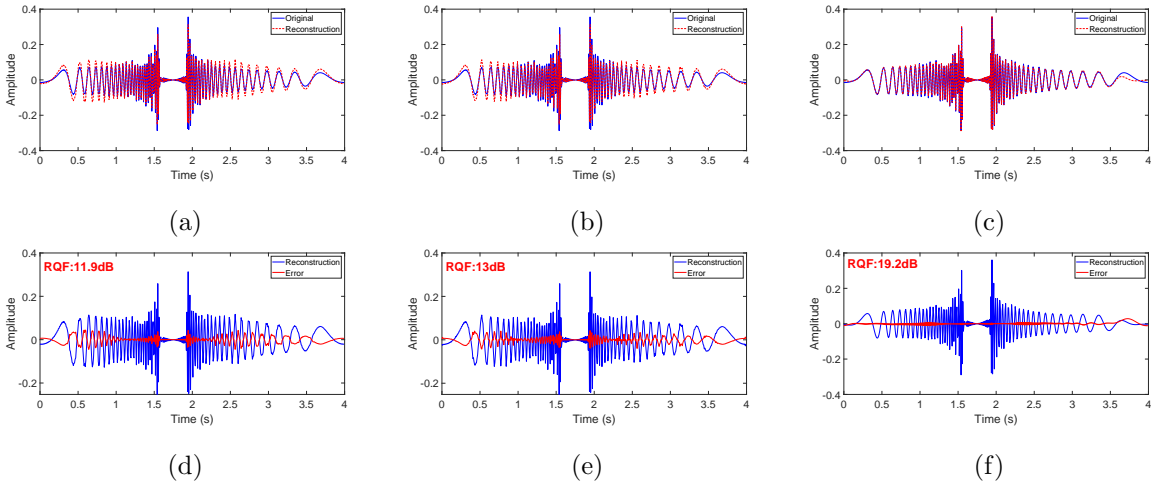


Figure 7: The original signal and reconstructed signals: (a) SWT, (b) MSWT, (c) TSST. The reconstructed signals and the reconstructed errors: (d) SWT, (e) MSWT, (f) TSST.

below the Rényi entropy curves of TSST2, MSWT and TSST, which means that the Rényi entropy values of NTEWT and RS are smaller. However, compared with RS reassigning along the time direction and frequency direction, NTEWT extracting only along the time direction has smaller Rényi entropies. It

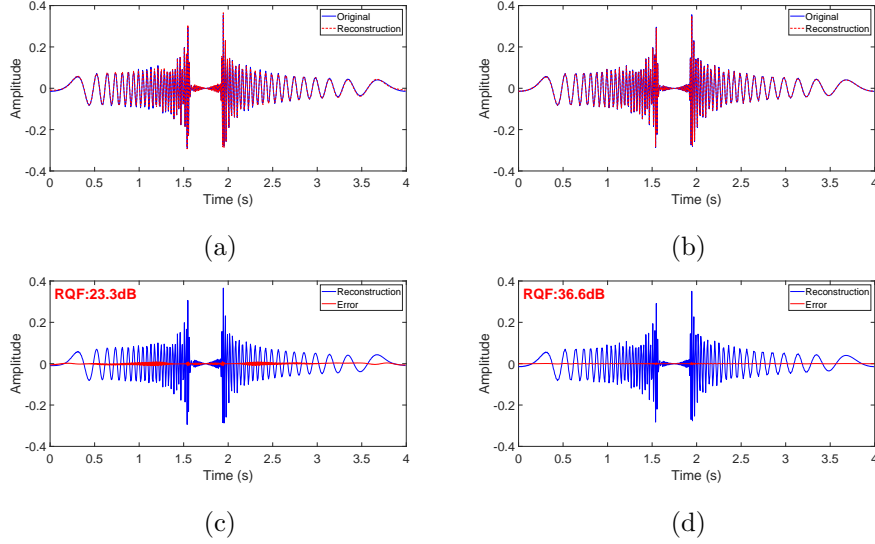


Figure 8: The original signal and reconstructed signals: (a) TSST2, (b) NTEWT. The reconstructed signals and the reconstructed errors: (c) TSST2, (d) NTEWT.

follows that among these TFA methods, NTEWT obtains the lowest Rényi entropy and behaves the best TF concentration performance whatever the noise level. Thus, NTEWT provides the most concentrated TFRs for analyzing noisy signals or noise-free signals.

Furthermore, we use the second quantified indicator, i.e., MRE, to evaluate the performance of NTEWT on detecting the GD feature of the signal, MRE can be employed to measure the errors of estimated GD, which is defined by [34],

$$\text{MRE} = \frac{1}{N_G} \left\| \frac{\widehat{\text{GD}} - \text{GD}}{\text{GD}} \right\|_1, \quad (43)$$

where $\|\cdot\|_1$ denotes l_1 -norm, N_G is the discrete length of the GD, GD and $\widehat{\text{GD}}$ respectively represent the true GD and the estimated GD. Generally, a lower MRE value means a better GD estimation performance. In Fig. 6, red lines denote true GD trajectory, blue lines denote estimated GD trajectories, and MRE values are written on both sides. As shown in Fig. 6, for two TFA post-processing methods along the frequency direction, the GD trajectory estimated by SWT deviates from the true GD trajectory most seriously, and as the second-order extension of SWT, MSWT reduces the deviation of both. However, for three TFA post-processing methods along the time direction, the GD trajectories estimated by TSST, TSST2 and NTEWT are closer to the true GD trajectory. Moreover, for RS along the frequency direction and the time direction, the GD trajectory estimated by RS is also very close to the true GD trajectory. It can be also seen that the GD trajectories estimated by the SWT, MSWT, TSST and TSST2 are interfered at high frequency, while the GD trajectories estimated by RS and NTEWT are almost unaffected at high frequency, and highly consistent with the true GD trajectory. And the MREs of GD estimated by RS and NTEWT are smaller than those of the other four TFA methods. Thus, RS and NTEWT shows better GD estimation performance.

Finally, the third quantified indicator RQF is used to evaluate the reconstruction performance, which is defined as [40]

$$RQF = 10 \log_{10} \frac{\|x(t)\|^2}{\|x(t) - x_r(t)\|^2}, \quad (44)$$

where $x(t)$ and $x_r(t)$ denote the original signal and the reconstructed signal, respectively. A higher RQF value indicates a better reconstruction performance. Figs. 7, 8 show reconstructed results of five TFA methods and their respective RQF values, and we find that the RQF values of TSST, TSST2 and NTEWT are lower than those of SWT and MSWT, and NTEWT achieves the smallest reconstruction error and the highest RQF value, it means that NTEWT behaves better reconstruction performance than other four reconstruction methods. Therefore, it can be concluded that, the TFA methods for post-processing operations along the time direction has more obvious advantages, in analyzing the strongly-varying signals in the frequency domain, than the TFA methods for post-processing operations along the frequency direction, especially the NTEWT behaves the best TF concentration, GD estimation and reconstruction performance for strongly frequency-varying signal $X(\omega)$ through three quantified indicators.

5.2. Application

In this subsection, we employ two real-world signals to validate the effectiveness of the proposed method. The first case is a popular bat signal recorded by Rice University [32], its waveform and spectrum are displayed in Fig. 9 (a), (b). We first use NTEWT to reconstruct the signal, and its reconstruction results are shown in Fig. 9 (c), (d). It can be seen that NTEWT can reconstruct signals well with high RQF value and with small reconstruction error, thus NTEWT behaves the good reconstruction ability. Furthermore, in order to understand the non-linear behaviors of the bat signal precisely, we use SWT, MSWT, RS, TSST, TSST2 and NTEWT to analyze the bat signal, and corresponding TF results are shown in Figs. 10, 11. Both the quantitative measure by the Rényi entropy and the visual interpretation show that the NTEWT can accurately characterize the bat signal and essentially improve the TF energy concentration of the bat signal.

Next, we consider a bearing vibration signal with the outer race fault, which was recorded by the Case Western Reserve University [41], and its waveform and spectrum are displayed in Fig. 12. As shown in Fig. 12 (b), the frequency band of this vibration signal is mainly concentrated in the frequency range of 2.5-4 kHz, thus we compare the TF features of this frequency range in Figs. 13, 14. Focus on the TF results and Rényi entropies, the NTEWT can provide a more concentrated TFR than other five TFA methods. This thus demonstrates the interest of the proposed new technique in real applications.

6. Conclusion

The main contribution of this paper is the introduction of Newton GD estimator and NTEWT, and its theoretical analysis. In this paper, we firstly convert the GD estimation problem into solving the fixed point problem, and combine with Newton algorithm to propose the Newton GD estimator for a

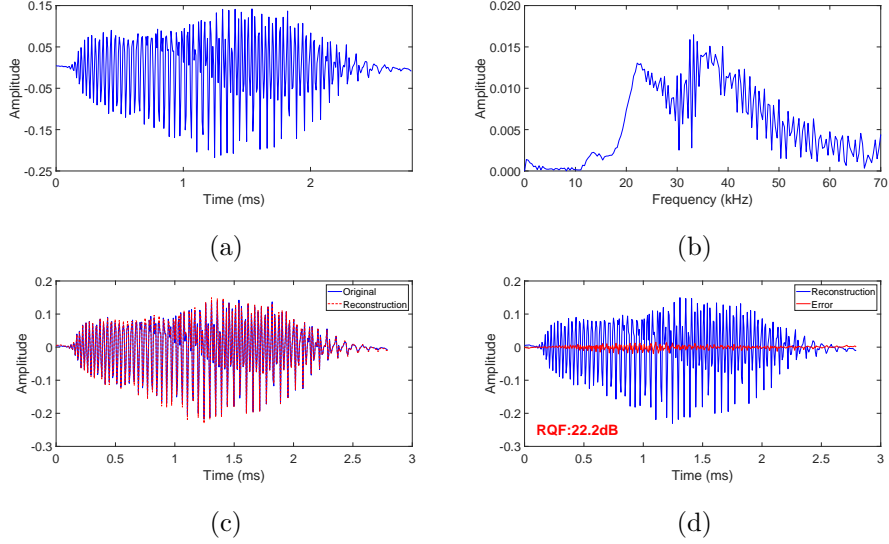


Figure 9: (a) The waveform of the bat signal. (b) The spectrum of the bat signal. (c) The original signal and the NTEWT reconstructed signal. (d) The reconstructed signal and the NTEWT reconstructed error.

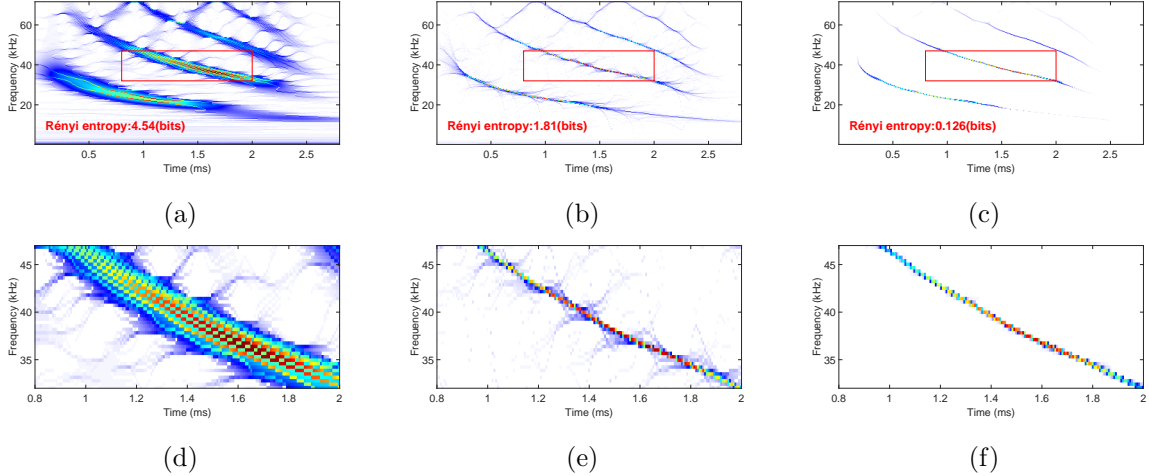


Figure 10: TF results for bat signal: (a) SWT, (b) MSWT, (c) RS, (d) zoom of the SWT, (e) zoom of the MSWT, (f) zoom of the RS.

frequency-varying linear chirp signal. Based on the Newton GD estimator, we then propose the NTEWT, which can achieve a high resolution TFR and reconstruct signal. Furthermore, we provide a precise mathematical definition for WFCC, and develop a comprehensive theoretical error analysis of NTEWT for WFCC, including approximate expression of WT, GD estimation and signal reconstruction. Finally, three quantitative indicators are used to compare NTEWT and other advanced TFA methods from the aspects of simulated and real signals. Both the quantitative indicators and the visual interpretation verify that the TFA post-processing methods along the time direction are more suitable for analyzing the strongly-varying signals in the frequency domain than the TFA post-processing methods along the frequency

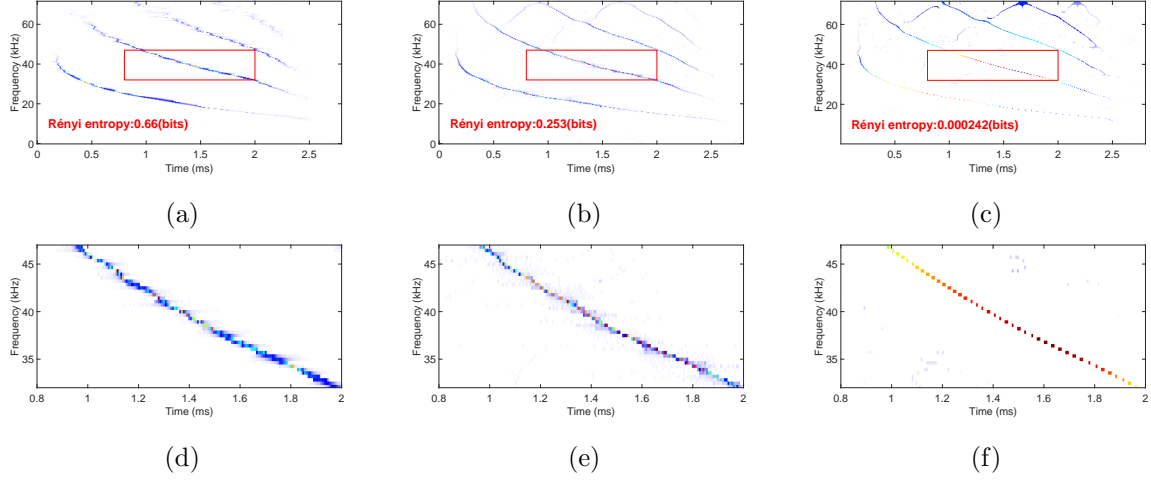


Figure 11: TF results for bat signal: (a) TSST, (b) TSST2, (c) NTEWT, (d) zoom of the TSST, (e) zoom of the TSST2, (f) zoom of the NTEWT.

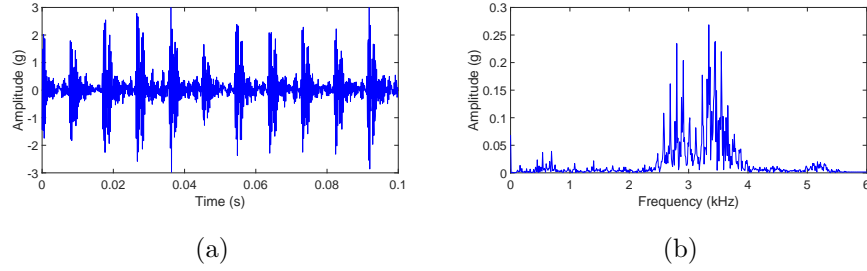


Figure 12: The waveform of vibration signal and its spectrum.

direction, especially the NTEWT has a more concentrated TFR, better GD estimation performance, and good reconstruction performance. In the future, we will try to develop a rigorous theoretical analysis of noise, and further explore the potential of the proposed method in practical applications.

Appendix A

For convenience, we divide the proof of Theorem 2 into several simple estimates and demonstrate one by one. The following lemma clearly explains the relationship between T_k satisfying weakly-separated condition and Z_k satisfying well-separated condition.

Lemma 3. For $k \in \{1, 2, \dots, K\}$, define a set Z_k

$$Z_k := \{(b, a); |\frac{\phi'_k(\frac{\omega_\psi}{a}) - b}{a}| < \Delta_k\}, \quad (45)$$

then the following hold:

- (1) $T_k \cap T_{k+1} = \emptyset$, $T_k \cap Z_{k+1} = \emptyset$ and $T_k \subset Z_k$.
- (2) If $d_{k,k+1} > \max\{\omega_\psi \Delta_k, \omega_\psi \Delta_{k+1}\}$, then $T_k \neq \emptyset$ with $(\phi'_k(\frac{\omega_\psi}{a}), a) \in T_k$.
- (3) If $d_{k,k+1} > \omega_\psi(\Delta_k + \Delta_{k+1})$, then $T_k = Z_k$.

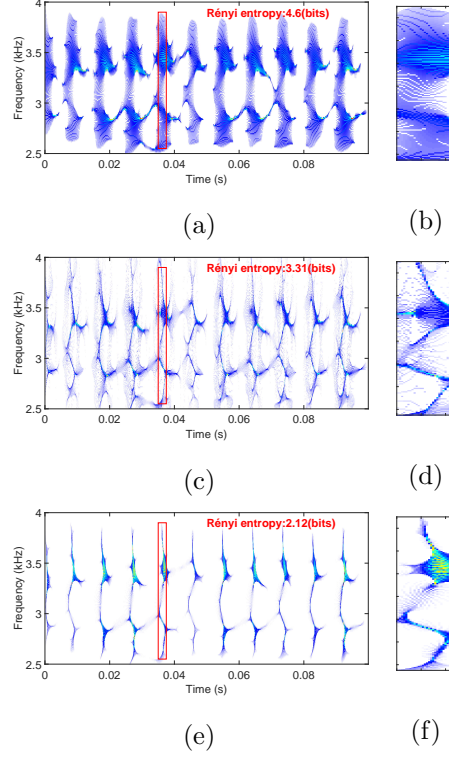


Figure 13: TF results for vibration signal: (a) SWT, (b) zoom of the SWT, (c) MSWT, (d) zoom of the MSWT, (e) RS, (f) zoom of the RS.

Proof. (1) On the one hand, based on Eq. (38), $\Pi^k(a)$ and $\Pi_{k+1}(a)$ can be written as

$$\begin{aligned}\Pi^k(a) &= \min\left\{\phi'_k\left(\frac{\omega_\psi}{a}\right) + a\Delta_k, \phi'_{k+1}\left(\frac{\omega_\psi}{a}\right) - a\Delta_{k+1}\right\}, \\ \Pi_{k+1}(a) &= \max\left\{\phi'_k\left(\frac{\omega_\psi}{a}\right) + a\Delta_k, \phi'_{k+1}\left(\frac{\omega_\psi}{a}\right) - a\Delta_{k+1}\right\},\end{aligned}\quad (46)$$

it is obvious that $\Pi^k(a) \leq \Pi_{k+1}(a)$, thus $T_k \cap T_{k+1} = \emptyset$. Combined with

$$\begin{aligned}\Pi^k(a) &\leq \phi'_{k+1}\left(\frac{\omega_\psi}{a}\right) - a\Delta_{k+1}, \\ Z_{k+1} &= \{(b, a); \phi'_{k+1}\left(\frac{\omega_\psi}{a}\right) - a\Delta_{k+1} < b < \phi'_{k+1}\left(\frac{\omega_\psi}{a}\right) + a\Delta_{k+1}\},\end{aligned}\quad (47)$$

it means that the lower boundary of the zones Z_{k+1} is above the upper boundary of the zones T_k , i.e. $T_k \cap Z_{k+1} = \emptyset$.

On the other hand, for any $(b, a) \in T_k$, i.e. $\Pi_k(a) < b < \Pi^k(a)$, combined with

$$b > \Pi_k(a) \geq \phi'_k\left(\frac{\omega_\psi}{a}\right) - a\Delta_k, \quad b < \Pi^k(a) \leq \phi'_k\left(\frac{\omega_\psi}{a}\right) + a\Delta_k, \quad (48)$$

this gives $(b, a) \in Z_k$, and $T_k \subset Z_k$.

(2) Since $X(\omega) = \sum_{k=1}^K X_k(\omega) \in \mathcal{C}_{\epsilon, d}$, $d_{k, k+1}$ satisfies the separation condition $\phi'_{k+1}\left(\frac{\omega_\psi}{a}\right) - \phi'_k\left(\frac{\omega_\psi}{a}\right) \geq \frac{ad_{k, k+1}}{\omega_\psi}$. When $d_{k, k+1} > \max\{\omega_\psi\Delta_k, \omega_\psi\Delta_{k+1}\}$, we have

$$\phi'_{k+1}\left(\frac{\omega_\psi}{a}\right) - \phi'_k\left(\frac{\omega_\psi}{a}\right) \geq \frac{ad_{k, k+1}}{\omega_\psi} > \max\{a\Delta_k, a\Delta_{k+1}\}, \quad (49)$$

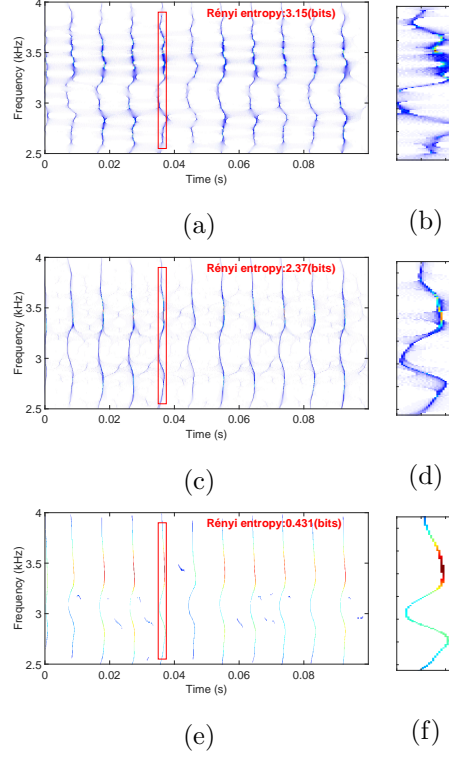


Figure 14: TF results for vibration signal: (a) TSST, (b) zoom of the TSST, (c) TSST2, (d) zoom of the TSST2, (e) NTEWT, (f) zoom of the NTEWT.

this gives

$$\phi'_{k+1}\left(\frac{\omega_\psi}{a}\right) > \phi'_k\left(\frac{\omega_\psi}{a}\right) + a\Delta_k, \quad \phi'_{k+1}\left(\frac{\omega_\psi}{a}\right) - a\Delta_{k+1} > \phi'_k\left(\frac{\omega_\psi}{a}\right). \quad (50)$$

Considering

$$\phi'_k\left(\frac{\omega_\psi}{a}\right) > \max\left\{\phi'_{k-1}\left(\frac{\omega_\psi}{a}\right) + a\Delta_{k-1}, \phi'_k\left(\frac{\omega_\psi}{a}\right) - a\Delta_k\right\} = \Pi_k(a), \quad (51)$$

and

$$\phi'_k\left(\frac{\omega_\psi}{a}\right) < \min\left\{\phi'_k\left(\frac{\omega_\psi}{a}\right) + a\Delta_k, \phi'_{k+1}\left(\frac{\omega_\psi}{a}\right) - a\Delta_{k+1}\right\} = \Pi^k(a), \quad (52)$$

leads to $(\phi'_k(\frac{\omega_\psi}{a}), a) \in T_k$, which means that $T_k \neq \emptyset$.

(3) According to separation condition and $d_{k,k+1} > \omega_\psi(\Delta_k + \Delta_{k+1})$, we have $\phi'_{k+1}(\frac{\omega_\psi}{a}) - \phi'_k(\frac{\omega_\psi}{a}) \geq \frac{ad_{k,k+1}}{\omega_\psi} > a(\Delta_k + \Delta_{k+1})$, which means that $\phi'_{k+1}(\frac{\omega_\psi}{a}) - a\Delta_{k+1} > \phi'_k(\frac{\omega_\psi}{a}) + a\Delta_k$. This leads to

$$\begin{aligned} \Pi_k(a) &= \max\left\{\phi'_{k-1}\left(\frac{\omega_\psi}{a}\right) + a\Delta_{k-1}, \phi'_k\left(\frac{\omega_\psi}{a}\right) - a\Delta_k\right\} = \phi'_k\left(\frac{\omega_\psi}{a}\right) - a\Delta_k, \\ \Pi^k(a) &= \min\left\{\phi'_k\left(\frac{\omega_\psi}{a}\right) + a\Delta_k, \phi'_{k+1}\left(\frac{\omega_\psi}{a}\right) - a\Delta_{k+1}\right\} = \phi'_k\left(\frac{\omega_\psi}{a}\right) + a\Delta_k. \end{aligned} \quad (53)$$

Thus, when $d_{k,k+1} > \omega_\psi(\Delta_k + \Delta_{k+1})$, we have $T_k = Z_k$. \square

The above lemma indicates that:

(1) Each zone T_k does not intersect with each other, T_k is a subset of Z_k . Moreover, T_k and Z_ℓ ($\ell \neq k$) don't intersect, which means that the zone T_k for component $X_k(\omega)$ is separated from the zone

Z_ℓ for other component $X_\ell(\omega)$, and it has been proved that in [38], Z_ℓ provides an estimate of the main energy distribution region of $W_{X_\ell}^{\hat{\psi}}(b, a)$.

(2) It is noteworthy that when $d_{k,k+1} > \max\{\omega_\psi \Delta_k, \omega_\psi \Delta_{k+1}\}$, weakly-separated chirp-like components of $\mathcal{C}_{\epsilon,d}$ may interfere with each other, and the zone T_k corresponds to the energy distribution region of $W_{X_k}^{\hat{\psi}}(b, a)$ of the k th component $X_k(\omega)$ at the point $(\phi'_k(\frac{\omega_\psi}{a}), a)$ and its vicinity.

(3) If $d_{k,k+1} > \omega_\psi(\Delta_k + \Delta_{k+1})$, then we have $T_k = Z_k$, it follows that weakly-separated conditions are restricted to well-separated cases, and the class $\mathcal{C}_{\epsilon,d}$ contains some signals with well-separated components.

In what follows, denote $M_k = \sup_{\omega \in \mathbb{R}} A_k(\omega) < \infty$, $M'_k = \max(\sup_{\omega \in \mathbb{R}} |A'_k(\omega)|, \sup_{\omega \in \mathbb{R}} \phi'_k(\omega)) < \infty$, $M''_k = \sup_{\omega \in \mathbb{R}} |\phi''_k(\omega)| < \infty$. If $O(A'_k)$ and $O(\phi''_k)$ are neglected, the k th component $X_k(\omega)$ can be approximated by Taylor expansion as

$$X_k(\omega) \approx \tilde{X}_k(\omega) = A_k\left(\frac{\omega_\psi}{a}\right) e^{-i[\phi_k(\frac{\omega_\psi}{a}) + \phi'_k(\frac{\omega_\psi}{a})(\omega - \frac{\omega_\psi}{a}) + \frac{1}{2}\phi''_k(\frac{\omega_\psi}{a})(\omega - \frac{\omega_\psi}{a})^2]}. \quad (54)$$

To simplify some notations, denote $t_k(b, a) = \frac{\phi'_k(\frac{\omega_\psi}{a}) - b}{\phi''_k(\frac{\omega_\psi}{a})}$. If $(b, a) \in T_k$, then $|t_k(b, a)| < \Delta_k$. Set $\Psi_k(t_k(b, a)) = \frac{\psi_{\phi''_k}^*(t_k(b, a))}{\psi_{\phi''_k}^*(t_k(b, a))}$, and for $(b, a) \in T_k$, assume

$$|\psi_{\phi''_k}(t_k(b, a))| \leq Q_k, \quad |\Psi_k(t_k(b, a))| \leq Q'_k, \quad |\Psi'_k(t_k(b, a))| \leq Q''_k. \quad (55)$$

Estimate 1. For each $k \in \{1, \dots, K\}$, we have

$$\begin{aligned} |A_k(\omega) - A_k\left(\frac{\omega_\psi}{a}\right)| &\leq \epsilon M''_k \left|\omega - \frac{\omega_\psi}{a}\right| \\ |\phi_k(\omega) - \phi_k\left(\frac{\omega_\psi}{a}\right) - \phi'_k\left(\frac{\omega_\psi}{a}\right)(\omega - \frac{\omega_\psi}{a}) - \frac{1}{2}\phi''_k\left(\frac{\omega_\psi}{a}\right)(\omega - \frac{\omega_\psi}{a})^2| &\leq \frac{1}{6}\epsilon M''_k \left|\omega - \frac{\omega_\psi}{a}\right|^3 \end{aligned} \quad (56)$$

Proof. When $\omega \geq \frac{\omega_\psi}{a}$, noticing Definition 10, we have (the case $\omega < \frac{\omega_\psi}{a}$ can be done in a similar way):

$$|A_k(\omega) - A_k\left(\frac{\omega_\psi}{a}\right)| = \left| \int_{\frac{\omega_\psi}{a}}^{\omega} A'_k(x) dx \right| \leq \int_{\frac{\omega_\psi}{a}}^{\omega} |A'_k(x)| dx \leq \epsilon \int_{\frac{\omega_\psi}{a}}^{\omega} |\phi''_k(x)| dx \leq \epsilon M''_k \left|\omega - \frac{\omega_\psi}{a}\right|, \quad (57)$$

On the other hand, it is easy to show that

$$\begin{aligned} |\phi_k(\omega) - \phi_k\left(\frac{\omega_\psi}{a}\right) - \phi'_k\left(\frac{\omega_\psi}{a}\right)(\omega - \frac{\omega_\psi}{a}) - \frac{1}{2}\phi''_k\left(\frac{\omega_\psi}{a}\right)(\omega - \frac{\omega_\psi}{a})^2| &= \left| \int_{\frac{\omega_\psi}{a}}^{\omega} \int_{\frac{\omega_\psi}{a}}^x [\phi''_k(y) - \phi''_k\left(\frac{\omega_\psi}{a}\right)] dy dx \right| \\ &= \left| \int_{\frac{\omega_\psi}{a}}^{\omega} \int_{\frac{\omega_\psi}{a}}^x \int_{\frac{\omega_\psi}{a}}^y \phi'''_k(\tau) d\tau dy dx \right| \leq \epsilon M''_k \int_{\frac{\omega_\psi}{a}}^{\omega} \int_{\frac{\omega_\psi}{a}}^x |y - \frac{\omega_\psi}{a}| dy dx = \frac{1}{6}\epsilon M''_k \left|\omega - \frac{\omega_\psi}{a}\right|^3. \quad \square \end{aligned} \quad (58)$$

Next, we will prove Theorem 2 (b) by approximating $\tilde{X}_k(\omega)$ to $X_k(\omega)$, which first needs to calculate several WTs of $\tilde{X}_k(\omega)$ and their upper bounds.

Estimate 2. (1) For each $k \in \{1, \dots, K\}$ and $(b, a) \in T_k$, we have

$$\begin{aligned} |W_{\tilde{X}_k}^{\hat{\psi}}(b, a)| &\leq \Upsilon_{0,0}(a), \quad |W_{\tilde{X}_k}^{\hat{\psi}'}(b, a)| \leq \Upsilon_{0,1}(a), \\ |\partial_b W_{\tilde{X}_k}^{\hat{\psi}}(b, a)| &\leq \Upsilon_{1,0}(a), \quad |\partial_b W_{\tilde{X}_k}^{\hat{\psi}'}(b, a)| \leq \Upsilon_{1,1}(a), \end{aligned} \quad (59)$$

where

$$\begin{aligned} \Upsilon_{0,0}(a) &= \frac{M_k Q_k}{2\pi a}, \quad \Upsilon_{0,1}(a) = \frac{M_k Q_k (\Delta_k + \frac{M''_k}{a^2} Q'_k)}{2\pi a}, \quad \Upsilon_{1,0}(a) = \frac{M_k Q_k (\omega_\psi + Q'_k)}{2\pi a^2}, \\ \Upsilon_{1,1}(a) &= \frac{M_k Q_k}{2\pi a^2} (1 + \Delta_k Q'_k + \Delta_k \omega_\psi + \frac{M''_k}{a^2} (\omega_\psi Q'_k + Q''_k + Q_k^2)). \end{aligned} \quad (60)$$

(2) Furthermore, for $(b, a) \in T_k$, for any $1 \leq \ell \neq k \leq K$, denote $\beta_\ell = \sup_{(b,a) \in \mathbb{R} \times \mathbb{R}^+} \{|t_\ell(b, a)|\}$, we have

$$\begin{aligned} |W_{\tilde{X}_\ell}^{\hat{\psi}}(b, a)| &\leq \epsilon J_{0,0}(a), \quad |W_{\tilde{X}_\ell}^{\hat{\psi}'}(b, a)| \leq \epsilon J_{0,1}(a) \\ |\partial_b W_{\tilde{X}_\ell}^{\hat{\psi}}(b, a)| &\leq \epsilon J_{1,0}(a), \quad |\partial_b W_{\tilde{X}_\ell}^{\hat{\psi}'}(b, a)| \leq \epsilon J_{1,1}(a) \end{aligned} \quad (61)$$

where

$$\begin{aligned} J_{0,0}(a) &= \frac{M_\ell G_0}{2\pi a}, \quad J_{0,1}(a) = \frac{M_\ell}{2\pi a^3} (a^2 G_0 \beta_\ell + G_1 M_\ell''), \quad J_{1,0}(a) = \frac{M_\ell}{2\pi a^2} (G_0 \omega_\psi + G_1), \\ J_{1,1}(a) &= \frac{M_\ell}{2\pi a^2} (G_0 + \omega_\psi (G_0 \beta_\ell + \frac{G_1 M_\ell''}{a^2}) + \beta_\ell G_1 + \frac{M_\ell'' G_2}{a^2}) \end{aligned} \quad (62)$$

Proof. (1) Based on Eqs. (5) and (54), the WT $W_{\tilde{X}_k}^{\hat{\psi}}(b, a)$ of $\tilde{X}_k(\omega)$ with $\hat{\psi}(\omega)$ can be expressed as

$$\begin{aligned} W_{\tilde{X}_k}^{\hat{\psi}}(b, a) &= \frac{1}{2\pi} \int_{\mathbb{R}} A_k\left(\frac{\omega_\psi}{a}\right) e^{-i[\phi_k(\frac{\omega_\psi}{a}) + \phi_k'(\frac{\omega_\psi}{a})(\omega - \frac{\omega_\psi}{a}) + \phi_k''(\frac{\omega_\psi}{a})\frac{(\omega - \frac{\omega_\psi}{a})^2}{2}]} \hat{\psi}^*(a\omega) e^{i\omega b} d\omega \\ &= \frac{1}{2\pi a} A_k\left(\frac{\omega_\psi}{a}\right) e^{-i\phi_k(\frac{\omega_\psi}{a})} e^{i\frac{\omega_\psi}{a} b} \int_{\mathbb{R}} e^{-i\phi_k''(\frac{\omega_\psi}{a})\frac{\omega^2}{2a^2}} \hat{\psi}^*(\omega + \omega_\psi) e^{-i(\phi_k'(\frac{\omega_\psi}{a}) - b)\frac{\omega}{a}} d\omega \\ &= \frac{1}{2\pi a} X_k\left(\frac{\omega_\psi}{a}\right) e^{i\frac{\omega_\psi}{a} b} \int_{\mathbb{R}} \hat{\psi}_\phi^*(\omega) e^{-i(\phi_k'(\frac{\omega_\psi}{a}) - b)\frac{\omega}{a}} d\omega \\ &= \frac{1}{2\pi a} X_k\left(\frac{\omega_\psi}{a}\right) e^{i\frac{\omega_\psi}{a} b} \psi_\phi^*(t_k(b, a)). \end{aligned} \quad (63)$$

Thus, $|W_{\tilde{X}_k}^{\hat{\psi}}(b, a)| \leq \frac{1}{2\pi a} M_k Q_k = \Upsilon_{0,0}(a)$. Furthermore, $W_{\tilde{X}_k}^{\hat{\psi}'}$, $\partial_b W_{\tilde{X}_k}^{\hat{\psi}}$ and $\partial_b W_{\tilde{X}_k}^{\hat{\psi}'}$ can be formulated as

$$\begin{aligned} W_{\tilde{X}_k}^{\hat{\psi}'}(b, a) &= \Lambda_{1,k}(a, b) W_{\tilde{X}_k}^{\hat{\psi}}(b, a), \quad \Lambda_{1,k}(a, b) = it_k(b, a) - \frac{\phi_k''(\frac{\omega_\psi}{a})}{a^2} \Psi(t_k(b, a)), \\ \partial_b W_{\tilde{X}_k}^{\hat{\psi}}(b, a) &= \Lambda_{2,k}(a, b) W_{\tilde{X}_k}^{\hat{\psi}}(b, a), \quad \Lambda_{2,k}(a, b) = i\frac{\omega_\psi}{a} - \frac{1}{a} \Psi(t_k(b, a)), \\ \partial_b W_{\tilde{X}_k}^{\hat{\psi}'}(b, a) &= \Lambda_{3,k}(a, b) W_{\tilde{X}_k}^{\hat{\psi}}(b, a), \\ \Lambda_{3,k}(a, b) &= -\left(\frac{i + it_k(b, a) \Psi(t_k(b, a)) + \omega_\psi t_k(b, a)}{a} + \frac{\phi_k''(\frac{\omega_\psi}{a})}{a^3} (i\omega_\psi \Psi(t_k(b, a)) - \Psi'(t_k(b, a)) - \Psi^2(t_k(b, a)))\right). \end{aligned} \quad (64)$$

From the above results, it is easy to obtain the bounds of these WTs.

(2) According to Lemma 3, for $(b, a) \in T_k$ and $k \neq \ell$, we have $T_k \cap Z_\ell = \emptyset$, and $(b, a) \notin Z_\ell$, i.e., $|t_\ell(b, a)| \geq \Delta_\ell$. According to the condition on $\psi_\phi(t)$, if $|t_\ell(b, a)| \geq \Delta_\ell$ with $d_{\ell, \ell+1} > \max\{\omega_\psi \Delta_\ell, \omega_\psi \Delta_{\ell+1}\}$, then $|\psi_\phi(t_\ell(b, a))| \leq \epsilon G_0$, $|\psi_\phi'(t_\ell(b, a))| \leq \epsilon G_1$, $|\psi_\phi''(t_\ell(b, a))| \leq \epsilon G_2$. Thus, by Eqs. (63) and (64), we obtain

$$|W_{\tilde{X}_\ell}^{\hat{\psi}}(b, a)| = \left| \frac{1}{2\pi a} X_\ell\left(\frac{\omega_\psi}{a}\right) e^{i\frac{\omega_\psi}{a} b} \psi_\phi^*(t_\ell(b, a)) \right| \leq \epsilon \frac{M_\ell G_0}{2\pi a} = \epsilon J_{0,0}(a), \quad (65)$$

$$\begin{aligned} |W_{\tilde{X}_\ell}^{\hat{\psi}'}(b, a)| &\leq |it_\ell(b, a) W_{\tilde{X}_\ell}^{\hat{\psi}}(b, a)| + \left| \frac{1}{2\pi a^3} X_\ell\left(\frac{\omega_\psi}{a}\right) e^{i\frac{\omega_\psi}{a} b} \phi_\ell''\left(\frac{\omega_\psi}{a}\right) \psi_\phi'^*(t_\ell(b, a)) \right| \\ &\leq \epsilon \beta_\ell \frac{M_\ell G_0}{2\pi a} + \epsilon \frac{M_\ell G_1}{2\pi a^3} M_\ell'' = \frac{\epsilon M_\ell}{2\pi a^3} (a^2 G_0 \beta_\ell + G_1 M_\ell'') = \epsilon J_{0,1}(a), \end{aligned} \quad (66)$$

$$\begin{aligned} |\partial_b W_{\tilde{X}_\ell}^{\hat{\psi}}(b, a)| &\leq \left| i\frac{\omega_\psi}{a} W_{\tilde{X}_\ell}^{\hat{\psi}}(b, a) \right| + \left| \frac{1}{2\pi a^2} X_\ell\left(\frac{\omega_\psi}{a}\right) e^{i\frac{\omega_\psi}{a} b} \psi_\phi'^*(t_\ell(b, a)) \right| \\ &\leq \epsilon \frac{M_\ell}{2\pi a^2} (G_0 \omega_\psi + G_1) = \epsilon J_{1,0}(a), \end{aligned} \quad (67)$$

and,

$$\begin{aligned}
|\partial_b W_{\tilde{X}_\ell}^{\hat{\psi}'}(b, a)| &\leq |i \frac{\omega_\psi}{a} W_{\tilde{X}_\ell}^{\hat{\psi}'}(b, a)| + |\frac{i}{a} W_{\tilde{X}_\ell}^{\hat{\psi}}(b, a)| \\
&+ |\frac{it_\ell(b, a)}{2\pi a^2} X_\ell(\frac{\omega_\psi}{a}) e^{i \frac{\omega_\psi}{a} b} \psi_\phi'^*(t_\ell(b, a))| + |\frac{\phi_\ell''(\frac{\omega_\psi}{a})}{2\pi a^4} X_\ell(\frac{\omega_\psi}{a}) e^{i \frac{\omega_\psi}{a} b} \psi_\phi''^*(t_\ell(b, a))| \\
&\leq \frac{\epsilon \omega_\psi M_\ell}{2\pi a^4} (a^2 G_0 \beta_\ell + G_1 M_\ell'') + \epsilon \frac{M_\ell G_0}{2\pi a^2} + \frac{\epsilon M_\ell \beta_\ell G_1}{2\pi a^2} + \frac{\epsilon M_\ell M_\ell'' G_2}{2\pi a^4} \\
&= \frac{\epsilon M_\ell}{2\pi a^2} (G_0 + \omega_\psi (G_0 \beta_\ell + \frac{G_1 M_\ell''}{a^2}) + \beta_\ell G_1 + \frac{M_\ell'' G_2}{a^2}) = \epsilon J_{1,1}(a). \quad \square
\end{aligned} \tag{68}$$

Estimate 3. For $k \in \{1, \dots, K\}$, and $(b, a) \in \mathbb{R} \times \mathbb{R}^+$, we have

$$\begin{aligned}
|W_{X_k}^{\hat{\psi}}(b, a) - W_{\tilde{X}_k}^{\hat{\psi}}(b, a)| &\leq \epsilon M_k'' (I_{0,0}^1(a) + \frac{M_k}{6} I_{0,0}^3(a)) \\
|W_{X_k}^{\hat{\psi}'}(b, a) - W_{\tilde{X}_k}^{\hat{\psi}'}(b, a)| &\leq \epsilon M_k'' (I_{0,1}^1(a) + \frac{M_k}{6} I_{0,1}^3(a)) \\
|\partial_b W_{X_k}^{\hat{\psi}}(b, a) - \partial_b W_{\tilde{X}_k}^{\hat{\psi}}(b, a)| &\leq \epsilon M_k'' (I_{1,0}^1(a) + \frac{M_k}{6} I_{1,0}^3(a)) \\
|\partial_b W_{X_k}^{\hat{\psi}'}(b, a) - \partial_b W_{\tilde{X}_k}^{\hat{\psi}'}(b, a)| &\leq \epsilon M_k'' (I_{1,1}^1(a) + \frac{M_k}{6} I_{1,1}^3(a)).
\end{aligned} \tag{69}$$

where $I_{p,q}^r(a) = \frac{1}{2\pi a^p} \int_{\mathbb{R}} |\omega - \frac{\omega_\psi}{a}|^r (a\omega)^p \hat{\psi}^{(q)}(a\omega) |d\omega$, $p, q = 0, 1$, $r = 1, 3$.

Proof. According to the WT definition, for $(b, a) \in \mathbb{R} \times \mathbb{R}^+$, we have

$$\begin{aligned}
|W_{X_k}^{\hat{\psi}}(b, a) - W_{\tilde{X}_k}^{\hat{\psi}}(b, a)| &\leq |\frac{1}{2\pi} \int_{\mathbb{R}} (A_k(\omega) - A_k(\frac{\omega_\psi}{a})) e^{-i\phi_k(\omega)} \hat{\psi}^*(a\omega) e^{i\omega b} d\omega| \\
&+ |\frac{1}{2\pi} \int_{\mathbb{R}} A_k(\frac{\omega_\psi}{a}) (e^{-i\phi_k(\omega)} - e^{-i[\phi_k(\frac{\omega_\psi}{a}) + \phi_k'(\frac{\omega_\psi}{a})(\omega - \frac{\omega_\psi}{a}) + \frac{1}{2}\phi_k''(\frac{\omega_\psi}{a})(\omega - \frac{\omega_\psi}{a})^2]}) \hat{\psi}^*(a\omega) e^{i\omega b} d\omega| \\
&\leq \frac{1}{2\pi} \int_{\mathbb{R}} |A_k(\omega) - A_k(\frac{\omega_\psi}{a})| |\hat{\psi}(a\omega)| d\omega \\
&+ \frac{1}{2\pi} \int_{\mathbb{R}} |A_k(\frac{\omega_\psi}{a})| |\phi_k(\omega) - \phi_k(\frac{\omega_\psi}{a}) - \phi_k'(\frac{\omega_\psi}{a})(\omega - \frac{\omega_\psi}{a}) - \frac{1}{2}\phi_k''(\frac{\omega_\psi}{a})(\omega - \frac{\omega_\psi}{a})^2| |\hat{\psi}(a\omega)| d\omega \\
&\leq \frac{\epsilon}{2\pi} M_k'' \int_{\mathbb{R}} |\omega - \frac{\omega_\psi}{a}| |\hat{\psi}(a\omega)| d\omega + \frac{\epsilon}{2\pi} \frac{1}{6} M_k M_k'' \int_{\mathbb{R}} |\omega - \frac{\omega_\psi}{a}|^3 |\hat{\psi}(a\omega)| d\omega \\
&\leq \epsilon M_k'' (I_{0,0}^1(a) + \frac{M_k}{6} I_{0,0}^3(a)),
\end{aligned} \tag{70}$$

where we use the differential mean value theorem $e^{ix} - e^{i0} = ie^{i\xi}x$ for the second inequality. The proofs of the other estimates are analogous. \square

Estimate 4. (1) For $k \in \{1, \dots, K\}$, and $(b, a) \in \mathbb{R} \times \mathbb{R}^+$, we have

$$\begin{aligned}
|W_X^{\hat{\psi}}(b, a) - \sum_{k=1}^K W_{\tilde{X}_k}^{\hat{\psi}}(b, a)| &\leq \epsilon \sum_{k=1}^K M_k'' (I_{0,0}^1(a) + \frac{M_k}{6} I_{0,0}^3(a)), \\
|W_X^{\hat{\psi}'}(b, a) - \sum_{k=1}^K W_{\tilde{X}_k}^{\hat{\psi}'}(b, a)| &\leq \epsilon \sum_{k=1}^K M_k'' (I_{0,1}^1(a) + \frac{M_k}{6} I_{0,1}^3(a)), \\
|\partial_b W_X^{\hat{\psi}}(b, a) - \sum_{k=1}^K \partial_b W_{\tilde{X}_k}^{\hat{\psi}}(b, a)| &\leq \epsilon \sum_{k=1}^K M_k'' (I_{1,0}^1(a) + \frac{M_k}{6} I_{1,0}^3(a)), \\
|\partial_b W_X^{\hat{\psi}'}(b, a) - \sum_{k=1}^K \partial_b W_{\tilde{X}_k}^{\hat{\psi}'}(b, a)| &\leq \epsilon \sum_{k=1}^K M_k'' (I_{1,1}^1(a) + \frac{M_k}{6} I_{1,1}^3(a)),
\end{aligned} \tag{71}$$

(2) Furthermore, for $(b, a) \in T_k$, we have

$$\begin{aligned} |W_X^{\hat{\psi}}(b, a) - W_{\tilde{X}_k}^{\hat{\psi}}(b, a)| &\leq \epsilon \Omega_{0,0}(a), \quad |W_X^{\hat{\psi}'}(b, a) - W_{\tilde{X}_k}^{\hat{\psi}'}(b, a)| \leq \epsilon \Omega_{0,1}(a) \\ |\partial_b W_X^{\hat{\psi}}(b, a) - \partial_b W_{\tilde{X}_k}^{\hat{\psi}}(b, a)| &\leq \epsilon \Omega_{1,0}(a), \quad |\partial_b W_X^{\hat{\psi}'}(b, a) - \partial_b W_{\tilde{X}_k}^{\hat{\psi}'}(b, a)| \leq \epsilon \Omega_{1,1}(a). \end{aligned} \quad (72)$$

where $\Omega_{p,q}(a) = \sum_{k=1}^K (M_k'' I_{p,q}^1(a) + \frac{M_k M_k''}{6} I_{p,q}^3(a) + J_{p,q}(a))$.

Proof. (1) According to Estimate 3, for $(b, a) \in \mathbb{R} \times \mathbb{R}^+$, we obtain

$$\begin{aligned} |W_X^{\hat{\psi}}(b, a) - \sum_{k=1}^K W_{\tilde{X}_k}^{\hat{\psi}}(b, a)| &\leq \sum_{k=1}^K |W_{\tilde{X}_k}^{\hat{\psi}}(b, a) - W_X^{\hat{\psi}}(b, a)| \\ &\leq \epsilon \sum_{k=1}^K (M_k'' I_{0,0}^1(a) + \frac{M_k}{6} I_{0,0}^3(a)). \end{aligned} \quad (73)$$

(2) For $(b, a) \in T_k$, according to Lemma 3, we have $(b, a) \notin Z_\ell$ ($\ell \neq k$), i.e. $|\frac{\phi_\ell'(\frac{\omega\psi}{a})-b}{a}| \geq \Delta_\ell$, then $|\psi_\phi(t_\ell(b, a))| \leq \epsilon G_0$. Thus, by Estimate 2 and Estimate 3, it follows that

$$\begin{aligned} |W_X^{\hat{\psi}}(b, a) - W_{\tilde{X}_k}^{\hat{\psi}}(b, a)| &\leq |\sum_{k=1}^K W_{\tilde{X}_k}^{\hat{\psi}}(b, a) - \sum_{k=1}^K W_{\tilde{X}_k}^{\hat{\psi}}(b, a)| + |\sum_{\ell \neq k}^K \tilde{W}_{\tilde{X}_\ell}^{\hat{\psi}}(b, a)| \\ &\leq \sum_{k=1}^K |W_{\tilde{X}_k}^{\hat{\psi}}(b, a) - W_X^{\hat{\psi}}(b, a)| + \epsilon \sum_{\ell \neq k}^K J_{0,0}(a) \\ &\leq \epsilon \sum_{k=1}^K (M_k'' I_{0,0}^1(a) + \frac{M_k M_k''}{6} I_{0,0}^3(a) + J_{0,0}(a)) = \epsilon \Omega_{0,0}(a). \end{aligned} \quad (74)$$

The proofs of the other estimates are analogous. \square

Estimate 5. For $k \in \{1, \dots, K\}$, and $(b, a) \in T_k$ for which holds $|W_X^{\hat{\psi}}(b, a)| > \tilde{\epsilon}$, we have

- (1) $|\tilde{t}_X(b, a) - \tilde{t}_{\tilde{X}_k}(b, a)| \leq \epsilon^{\frac{3}{4}} \Gamma_0(a)$, where $\Gamma_0(a) = a(\Omega_{0,1}(a) + (\Delta_k + \frac{M_k''}{a^2} Q'_k) \Omega_{0,0}(a))$.
- (2) $|\partial_b \tilde{t}_X(b, a) - \partial_b \tilde{t}_{\tilde{X}_k}(b, a)| \leq \epsilon^{\frac{1}{2}} \Gamma_1(a)$, where

$$\begin{aligned} \Gamma_1(a) &= a(\epsilon^{\frac{1}{4}} \Omega_{1,1}(a) + \Upsilon_{1,1}(a) \Omega_{0,0}(a) + (\epsilon \Omega_{1,0}(a) + \Upsilon_{1,0}(a)) \Omega_{0,1}(a) \\ &\quad + \Upsilon_{0,1}(a) \Omega_{1,0}(a) + (1 + \frac{1}{a^2} M_k'' Q_k'') (\epsilon \Omega_{0,0}(a) + 2 \Upsilon_{0,0}(a)) \Omega_{0,0}(a)). \end{aligned} \quad (75)$$

Proof. (1) Based on Eqs. (19), (64) and (72), we obtain

$$\begin{aligned} |\tilde{t}_X(b, a) - \tilde{t}_{\tilde{X}_k}(b, a)| &= |ia \frac{W_X^{\hat{\psi}'}(b, a)}{W_X^{\hat{\psi}}(b, a)} - \Lambda_{1,k}(a, b)| = |ia \frac{W_X^{\hat{\psi}'}(b, a) - \Lambda_{1,k}(a, b) W_X^{\hat{\psi}}(b, a)}{W_X^{\hat{\psi}}(b, a)}| \\ &= |ia \frac{(W_X^{\hat{\psi}'}(b, a) - W_{\tilde{X}_k}^{\hat{\psi}'}(b, a)) + (W_{\tilde{X}_k}^{\hat{\psi}'}(b, a) - \Lambda_{1,k}(a, b) W_{\tilde{X}_k}^{\hat{\psi}}(b, a)) + \Lambda_{1,k}(a, b) (W_{\tilde{X}_k}^{\hat{\psi}}(b, a) - W_X^{\hat{\psi}}(b, a))}{W_X^{\hat{\psi}}(b, a)}| \\ &\leq |ia \frac{W_X^{\hat{\psi}'}(b, a) - W_{\tilde{X}_k}^{\hat{\psi}'}(b, a)}{W_X^{\hat{\psi}}(b, a)}| + |ia \frac{\Lambda_{1,k}(a, b) (W_{\tilde{X}_k}^{\hat{\psi}}(b, a) - W_X^{\hat{\psi}}(b, a))}{W_X^{\hat{\psi}}(b, a)}| \\ &\leq \epsilon^{\frac{3}{4}} a (\Omega_{0,1}(a) + |\Lambda_{1,k}(a, b)| \Omega_{0,0}(a)) \leq \epsilon^{\frac{3}{4}} a (\Omega_{0,1}(a) + (\Delta_k + \frac{M_k''}{a^2} Q'_k) \Omega_{0,0}(a)) = \epsilon^{\frac{3}{4}} \Gamma_0(a) \end{aligned} \quad (76)$$

(2) By Eq. (19), we have

$$\partial_b \tilde{t}_{\tilde{X}_k}(b, a) = 1 - ia \left(\frac{\partial_b W_{\tilde{X}_k}^{\psi'}(b, a) W_{\tilde{X}_k}^{\psi}(b, a) - W_{\tilde{X}_k}^{\psi'}(b, a) \partial_b W_{\tilde{X}_k}^{\psi}(b, a)}{(W_{\tilde{X}_k}^{\psi}(b, a))^2} \right), \quad (77)$$

this gives

$$(1 - \partial_b \tilde{t}_{\tilde{X}_k}(b, a))(W_{\tilde{X}_k}^{\psi}(b, a))^2 = ia(\partial_b W_{\tilde{X}_k}^{\psi'}(b, a) W_{\tilde{X}_k}^{\psi}(b, a) - W_{\tilde{X}_k}^{\psi'}(b, a) \partial_b W_{\tilde{X}_k}^{\psi}(b, a)),$$

then, we can get

$$\begin{aligned} |\partial_b \tilde{t}_X(b, a) - \partial_b \tilde{t}_{\tilde{X}_k}(b, a)| &= \left| 1 - ia \left(\frac{\partial_b W_X^{\psi'}(b, a) W_X^{\psi}(b, a) - W_X^{\psi'}(b, a) \partial_b W_X^{\psi}(b, a)}{(W_X^{\psi}(b, a))^2} \right) - \partial_b \tilde{t}_{\tilde{X}_k}(b, a) \right| \\ &\leq \left| \frac{ia(\partial_b W_X^{\psi'}(b, a) W_X^{\psi}(b, a) - W_X^{\psi'}(b, a) \partial_b W_X^{\psi}(b, a) - (\partial_b W_{\tilde{X}_k}^{\psi'}(b, a) W_{\tilde{X}_k}^{\psi}(b, a) - W_{\tilde{X}_k}^{\psi'}(b, a) \partial_b W_{\tilde{X}_k}^{\psi}(b, a)))}{(W_X^{\psi}(b, a))^2} \right| \\ &+ \left| \frac{(1 - \partial_b \tilde{t}_{\tilde{X}_k}(b, a))((W_X^{\psi}(b, a))^2 - (W_{\tilde{X}_k}^{\psi}(b, a))^2)}{(W_X^{\psi}(b, a))^2} \right| \\ &\leq \left| a \frac{\partial_b W_X^{\psi'}(b, a) - \partial_b W_{\tilde{X}_k}^{\psi'}(b, a)}{W_X^{\psi}(b, a)} \right| + \left| a \frac{\partial_b W_{\tilde{X}_k}^{\psi'}(b, a) (W_X^{\psi}(b, a) - W_{\tilde{X}_k}^{\psi}(b, a))}{(W_X^{\psi}(b, a))^2} \right| + \left| a \frac{(W_X^{\psi'}(b, a) - W_{\tilde{X}_k}^{\psi'}(b, a)) \partial_b W_X^{\psi}(b, a)}{(W_X^{\psi}(b, a))^2} \right| \\ &+ \left| a \frac{W_{\tilde{X}_k}^{\psi'}(b, a) (\partial_b W_X^{\psi}(b, a) - \partial_b W_{\tilde{X}_k}^{\psi}(b, a))}{(W_X^{\psi}(b, a))^2} \right| + \left| \frac{(1 - \partial_b \tilde{t}_{\tilde{X}_k}(b, a))((W_X^{\psi}(b, a))^2 - (W_{\tilde{X}_k}^{\psi}(b, a))^2)}{(W_X^{\psi}(b, a))^2} \right| \\ &\leq a \epsilon^{\frac{3}{4}} \Omega_{1,1}(a) + a \epsilon^{\frac{1}{2}} |\partial_b W_{\tilde{X}_k}^{\psi'}(b, a)| \Omega_{0,0}(a) + a \epsilon^{\frac{1}{2}} |\partial_b W_X^{\psi'}(b, a)| \Omega_{0,1}(a) + a \epsilon^{\frac{1}{2}} |W_{\tilde{X}_k}^{\psi'}(b, a)| \Omega_{1,0}(a) \\ &+ a \epsilon^{\frac{1}{2}} |1 - \partial_b \tilde{t}_{\tilde{X}_k}(b, a)| |W_X^{\psi}(b, a) + W_{\tilde{X}_k}^{\psi}(b, a)| \Omega_{0,0}(a) \end{aligned} \quad (78)$$

According to Eq. (7), $\tilde{t}_{X_k}(b, a)$ and $\partial_b \tilde{t}_{X_k}(b, a)$ can be formulated as

$$\tilde{t}_{X_k}(b, a) = \phi'_k \left(\frac{\omega_\psi}{a} \right) + i \frac{\phi''_k \left(\frac{\omega_\psi}{a} \right)}{a} \Psi(t_k(b, a)), \quad \partial_b \tilde{t}_{X_k}(b, a) = -i \frac{\phi''_k \left(\frac{\omega_\psi}{a} \right)}{a^2} \Psi'(t_k(b, a)). \quad (79)$$

Also note that $|\Psi'_k(t_k(b, a))| \leq Q''_k$, it follows that

$$|1 - \partial_b \tilde{t}_{\tilde{X}_k}(b, a)| \leq 1 + |\partial_b \tilde{t}_{\tilde{X}_k}(b, a)| \leq 1 + \frac{1}{a^2} M''_k Q''_k. \quad (80)$$

By Estimate 2 and Estimate 4, considering that

$$|\partial_b W_X^{\psi}(b, a)| \leq |\partial_b W_X^{\psi}(b, a) - \partial_b W_{\tilde{X}_k}^{\psi}(b, a)| + |\partial_b W_{\tilde{X}_k}^{\psi}(b, a)| \leq \epsilon \Omega_{1,0}(a) + \Upsilon_{1,0}(a), \quad (81)$$

and,

$$|W_X^{\psi}(b, a) + W_{\tilde{X}_k}^{\psi}(b, a)| \leq |W_X^{\psi}(b, a) - W_{\tilde{X}_k}^{\psi}(b, a)| + 2|W_{\tilde{X}_k}^{\psi}(b, a)| \leq \epsilon \Omega_{0,0}(a) + 2\Upsilon_{0,0}(a), \quad (82)$$

it leads to

$$\begin{aligned} |\partial_b \tilde{t}_X(b, a) - \partial_b \tilde{t}_{\tilde{X}_k}(b, a)| &\leq a \epsilon^{\frac{1}{2}} (\epsilon^{\frac{1}{4}} \Omega_{1,1}(a) + \Upsilon_{1,1}(a) \Omega_{0,0}(a) + (\epsilon \Omega_{1,0}(a) + \Upsilon_{1,0}(a)) \Omega_{0,1}(a) + \Upsilon_{0,1}(a) \Omega_{1,0}(a)) \\ &+ \left(1 + \frac{1}{a^2} M''_k Q''_k \right) (\epsilon \Omega_{0,0}(a) + 2\Upsilon_{0,0}(a)) \Omega_{0,0}(a) = \epsilon^{\frac{1}{2}} \Gamma_1(a). \quad \square \end{aligned} \quad (83)$$

Next, we will consider the error analysis of the Newton GD estimator and the true GD.

Estimate 6. For $k \in \{1, \dots, K\}$, and $(b, a) \in T_k$ such that $|W_{\tilde{X}}^{\psi}(b, a)| > \tilde{\epsilon}$, we have

(1) Denote $P_k = \inf_{a \in \mathbb{R}^+} \{|1 + i \frac{\phi_k''(\frac{\omega\psi}{a})}{a^2} \Psi'(t_k(b, a))|\}$, if there exists some constant S_k such that $|\Psi(t_k(b, a)) - t_k(b, a) \Psi'(t_k(b, a))| \leq \epsilon S_k$, then

$$|\bar{t}_{\tilde{X}_k}(b, a) - \phi_k'(\frac{\omega\psi}{a})| \leq \epsilon \frac{M_k'' S_k}{a P_k}. \quad (84)$$

(2) Furthermore, we have

$$|\bar{t}_X(b, a) - \phi_k'(\frac{\omega\psi}{a})| \leq \epsilon^{\frac{1}{2}} \Gamma_2(a), \quad (85)$$

where $\Gamma_2(a) = \frac{\epsilon^{\frac{1}{4}} \Gamma_0(a) + a \Delta_k \Gamma_1(a) + \epsilon^{\frac{1}{2}} \frac{M_k'' S_k}{a P_k} (H + \epsilon^{\frac{1}{2}} \Gamma_1(a))}{H}$, with $H = \inf_{a \in \mathbb{R}^+} \{|1 - \partial_b \tilde{t}_X(b, a)|\}$.

Proof. (1) By Eq. (32), we have

$$\begin{aligned} |\bar{t}_{\tilde{X}_k}(b, a) - \phi_k'(\frac{\omega\psi}{a})| &= |b - \frac{b - \phi_k'(\frac{\omega\psi}{a}) - i \frac{\phi_k''(\frac{\omega\psi}{a})}{a} \Psi(t_k(b, a))}{1 + i \frac{\phi_k''(\frac{\omega\psi}{a})}{a^2} \Psi'(t_k(b, a))} - \phi_k'(\frac{\omega\psi}{a})| \\ &\leq \left| \frac{i \frac{\phi_k''(\frac{\omega\psi}{a})}{a} (\Psi(t_k(b, a)) - t_k(b, a) \Psi'(t_k(b, a)))}{1 + i \frac{\phi_k''(\frac{\omega\psi}{a})}{a^2} \Psi'(t_k(b, a))} \right| \leq \epsilon \frac{M_k'' S_k}{a P_k}. \end{aligned} \quad (86)$$

2) According to the definition of $\bar{t}_X(b, a)$, we have then

$$\begin{aligned} |\bar{t}_X(b, a) - \phi_k'(\frac{\omega\psi}{a})| &= |b - \frac{b - \tilde{t}_X(b, a)}{1 - \partial_b \tilde{t}_X(b, a)} - \phi_k'(\frac{\omega\psi}{a})| = \left| \frac{b - \tilde{t}_X(b, a) - (b - \phi_k'(\frac{\omega\psi}{a}))(1 - \partial_b \tilde{t}_X(b, a))}{1 - \partial_b \tilde{t}_X(b, a)} \right| \\ &\leq \left| \frac{b - \tilde{t}_X(b, a) - (b - \tilde{t}_{\tilde{X}_k}(b, a))}{1 - \partial_b \tilde{t}_X(b, a)} \right| + \left| \frac{(b - \phi_k'(\frac{\omega\psi}{a}))(1 - \partial_b \tilde{t}_X(b, a)) - (b - \phi_k'(\frac{\omega\psi}{a}))(1 - \partial_b \tilde{t}_{\tilde{X}_k}(b, a))}{1 - \partial_b \tilde{t}_X(b, a)} \right| \\ &+ \left| \frac{b - \tilde{t}_{\tilde{X}_k}(b, a) - (b - \phi_k'(\frac{\omega\psi}{a}))(1 - \partial_b \tilde{t}_{\tilde{X}_k}(b, a))}{1 - \partial_b \tilde{t}_X(b, a)} \right| \\ &\leq \left| \frac{\tilde{t}_X(b, a) - \tilde{t}_{\tilde{X}_k}(b, a)}{1 - \partial_b \tilde{t}_X(b, a)} \right| + \left| \frac{(b - \phi_k'(\frac{\omega\psi}{a}))(1 - \partial_b \tilde{t}_X(b, a)) - (b - \phi_k'(\frac{\omega\psi}{a}))(1 - \partial_b \tilde{t}_{\tilde{X}_k}(b, a))}{1 - \partial_b \tilde{t}_X(b, a)} \right| + \left| \frac{(\tilde{t}_{\tilde{X}_k}(b, a) - \phi_k'(\frac{\omega\psi}{a}))(1 - \partial_b \tilde{t}_{\tilde{X}_k}(b, a))}{1 - \partial_b \tilde{t}_X(b, a)} \right| \\ &\leq \frac{\epsilon^{\frac{1}{2}}}{H} (\epsilon^{\frac{1}{4}} \Gamma_0(a) + a \Delta_k \Gamma_1(a) + \epsilon^{\frac{1}{2}} \frac{M_k'' S_k}{a P_k} (H + \epsilon^{\frac{1}{2}} \Gamma_1(a))) = \epsilon^{\frac{1}{2}} \Gamma_2(a). \end{aligned} \quad (87)$$

where the last inequality uses $\left| \frac{1 - \partial_b \tilde{t}_{\tilde{X}_k}(b, a)}{1 - \partial_b \tilde{t}_X(b, a)} \right| = \left| 1 + \frac{\partial_b \tilde{t}_X(b, a) - \partial_b \tilde{t}_{\tilde{X}_k}(b, a)}{1 - \partial_b \tilde{t}_X(b, a)} \right| \leq \frac{1}{H} (H + \epsilon^{\frac{1}{2}} \Gamma_1(a))$. \square

Proof of Theorem 2 (b). Assume $\epsilon^{\frac{1}{4}} \Gamma_2(a) < 1$, then we have

$$|\bar{t}_X(b, a) - \phi_k'(\frac{\omega\psi}{a})| \leq \tilde{\epsilon}. \quad \square \quad (88)$$

Proof of Theorem 2 (c). For $(b, a) \in T_k$, we evaluate the WT in Eq. (63) along the trajectory $b = \phi_k'(\frac{\omega\psi}{a})$

$$W_{\tilde{X}_k}^{\psi}(\phi_k'(\frac{\omega\psi}{a}), a) = \frac{1}{2\pi a} X_k(\frac{\omega\psi}{a}) e^{i \frac{\omega\psi}{a} \phi_k'(\frac{\omega\psi}{a})} \psi_{\phi}^*(0), \quad (89)$$

it follows that,

$$X_k(\frac{\omega\psi}{a}) = \frac{2\pi a W_{\tilde{X}_k}^{\psi}(\phi_k'(\frac{\omega\psi}{a}), a) e^{-i \frac{\omega\psi}{a} \phi_k'(\frac{\omega\psi}{a})}}{\psi_{\phi}^*(0)}. \quad (90)$$

According to Estimate 4, we have

$$\begin{aligned}
& \left| \frac{2\pi a N T e(\phi'_k(\frac{\omega_\psi}{a}), a) e^{-i\frac{\omega_\psi}{a} \phi'_k(\frac{\omega_\psi}{a})}}{\psi_\phi^*(0)} - X_k(\frac{\omega_\psi}{a}) \right| \\
& \leq \left| \frac{2\pi a}{\psi_\phi^*(0)} |W_{\hat{X}}^{\hat{\psi}}(\phi'_k(\frac{\omega_\psi}{a}), a) - W_{\tilde{X}_k}^{\hat{\psi}}(\phi'_k(\frac{\omega_\psi}{a}), a)| \right| + \left| \frac{2\pi a W_{\tilde{X}_k}^{\hat{\psi}}(\phi'_k(\frac{\omega_\psi}{a}), a) e^{-i\frac{\omega_\psi}{a} \phi'_k(\frac{\omega_\psi}{a})}}{\psi_\phi^*(0)} - X_k(\frac{\omega_\psi}{a}) \right| \quad (91) \\
& \leq \epsilon \left| \frac{2\pi a}{\psi_\phi(0)} \right| \Omega_{0,0}(a) = C\tilde{\epsilon}.
\end{aligned}$$

The proof of Theorem 2 is finished. \square

Acknowledgements

This work was supported by National Natural Science Foundation of China under Grant U20B2075, supported by the ANR ASCETE project with Grant number ANR-19-CE48-0001-01, supported by the Fundamental Research Funds for the Central Universities under Grant G2021KY05103, and supported by the Natural Science Foundation of Shaanxi Province under Grant 2023-JC-QN-0739. The authors thank the editor and the anonymous reviewers for their valuable comments and suggestions that helped improve the quality of this paper.

Data availability statement

The authors do not have permission to share data.

References

- [1] L. Cohen., Time-frequency analysis: theory and applications. Englewood Cliffs, NJ, USA: Prentice-Hall, 1995.
- [2] M. G. Amin, Y. D. Zhang, F. Ahmad, Radar signal processing for elderly fall detection: the future for in-home monitoring, *IEEE Signal Process. Mag.* 33 (2) (2016) 71-80.
- [3] S. Fomel., Seismic data decomposition into spectral components using regularized nonstationary autoregression, *Geophysics.* 78 (6) (2013) 069-076.
- [4] C. Park, D. Looney, P. Kidmose, M. Ungstrup, D.P. Mandic., Time-frequency analysis of EEG asymmetry using bivariate empirical mode decomposition, *IEEE Trans. Neural Syst. Rehabil. Eng.* 19 (4) (2011) 366-373.
- [5] H. Yang., Synchrosqueezed wave packet transforms and diffeomorphism based spectral analysis for 1D general mode decompositions, *Appl. Computat. Harmon. Anal.* 39 (1) (2015) 33-66.
- [6] X. Zhu, Z. Zhang, J. Gao, W. Li., Two robust approaches to multicomponent signal reconstruction from STFT ridges, *Mech. Syst. Signal Process.* 115 (2019) 720-735.

- [7] S. Wang, X. Chen, I. W. Selesnick, Y. Guo, C. Tong, X. Zhang., Matching synchrosqueezing transform: a useful tool for characterizing signals with fastvarying instantaneous frequency and application to machine fault diagnosis, *Mech. Syst. Signal Process.* 100 (2018) 242-288.
- [8] S. Mallat., *A wavelet tour of signal processing: the sparse way* (3rd edn). Acad. Press, Burlington, 2009.
- [9] P. Flandrin., *Time-frequency/time-scale analysis*. Acad. Press, 1998.
- [10] S. Mann, S. Haykin, The chirplet transform: physical considerations, *IEEE Trans. Signal Process.* 43 (1) (1995) 2745-2761.
- [11] X. Li, G. Bi, S. Stankovic, et al, Local polynomial Fourier transform: a review on recent developments and applications, *Signal Process.* 91 (6) (2011) 1370-1393.
- [12] S. Wang, X. Chen, G. Cai, B. Chen, X. Li, Z. He, Matching demodulation transform and synchrosqueezing in time-frequency analysis, *IEEE Trans. Signal Process.* 62 (1) (2014) 69-84.
- [13] K. Kodera, C. de Villedary, and R. Gendrin., A new method for the numerical analysis of nonstationary signals, *Phys. Earth and Plan. Int.* 12 (2-3) (1976) 142-150.
- [14] K. Kodera, R. Gendrin, and C. de Villedary., Analysis of time-varying signals with small BT values, *IEEE Trans. Acoust., Speech, Signal Process., ASSP.* 26 (1) (1978) 64-76.
- [15] F. Auger and P. Flandrin., Improving the readability of time-frequency and time-scale representations by the reassignment method, *IEEE Trans. Signal Process.* 43 (5) (1995) 1068-1089.
- [16] P. Flandrin, F. Auger, and E. Chassande-Mottin., Time-frequency reassignment: from principles to algorithms, *Applications in Time-Frequency Signal Processing.* (2003) 179-203.
- [17] E. Chassande-Mottin, F. Auger, and P. Flandrin., Time frequency/time-scale reassignment, *Wavelets and signal processing.* (2003) 233-267.
- [18] E. Chassande-Mottin, I. Daubechies, F. Auger, and P. Flandrin., Differential reassignment, *IEEE Signal Process. Lett.* 4 (10) (1997) 293-294.
- [19] I. Daubechies and S. Maes., A nonlinear squeezing of the continuous wavelet transform, *Wavelets in Medicine and Bio.* (1996) 527-546.
- [20] N.E. Huang, Z. Shen, S.R. Long, M.L. Wu, H.H. Shih, Q. Zheng, N.C. Yen, C.C. Tung, and H.H. Liu, The empirical mode decomposition and Hilbert spectrum for nonlinear and non-stationary time series analysis, *Proc. Roy. Soc., London A*, 454 (1998) 903-995.
- [21] Dragomiretskiy. K, Zosso. D. Variational mode decomposition, *IEEE Trans. Signal Process*, 62 (3) (2014) 531-544.

- [22] Gilles J. Empirical wavelet transform, *IEEE Trans. Signal Process*, 61 (16) (2013) 3999-4010.
- [23] I. Daubechies, J. Lu, and H.T. Wu., Synchrosqueezed wavelet transforms: an empirical mode decomposition-like tool, *Appl. Comp. Harmonic Anal.* 30 (2) (2011) 243-261.
- [24] F. Auger, P. Flandrin, Y-T Lin, S. McLaughlin, S. Meignen, T. Oberlin, and H.T. Wu, Time-frequency reassignment and synchrosqueezing: an overview, *IEEE Signal Process. Mag.* 30 (6) (2013) 32-41.
- [25] F. Auger, E. Chassande-Mottin, and P. Flandrin, On phase-magnitude relationships in the short-time Fourier transform, *IEEE Signal Process. Lett.*, 19 (5) 2012 (267-270) .
- [26] J. Brynolfsson, M. Sandsten., Parameter estimation of oscillating Gaussian functions using the scaled reassigned spectrogram, *Signal Process.* 150 (2018) 20-32.
- [27] T. Oberlin, S. Meignen, and V. Perrier., Second-order synchrosqueezing transform or invertible reassignment? Towards ideal time-frequency representations, *IEEE Trans. Signal Process.* 63 (5) (2015) 1335-1344.
- [28] D. Fourer, F. Auger, K. Czarnecki, S. Meignen, and P. Flandrin., Chirp rate and instantaneous frequency estimation: application to recursive vertical synchrosqueezing, *IEEE Signal Process. Lett.* 24 (11) (2017) 1724-1728.
- [29] G. Yu, Z. Wang, P. Zhao, Z. Li., Local maximum synchrosqueezing transform: an energy-concentrated time-frequency analysis tool, *Mech Syst. Signal Process.* 117 (2019) 537-552.
- [30] G. Yu, Z. Wang, P. Zhao., Multi-synchrosqueezing transform, *IEEE Trans. Ind. Electron.* 66 (7) (2019) 5441-5455.
- [31] L. Li, H. Cai, Q. Jiang., Adaptive synchrosqueezing transform with a time-varying parameter for nonstationary signal separation, *Appl. Comput. Harmon. Anal.* 49 (2020) 1075-1106.
- [32] G. Yu, M. Yu and C. X., Synchroextracting transform, *IEEE Trans. Ind. Electron.* 64 (10) (2017) 8042-8054.
- [33] W. Bao, F. Li, X. Tu, Y. Hu, Z. He., Second-order synchroextracting transform with application to fault diagnosis, *IEEE Transactions on Instrumentation and Measurement.* 70 (2020) 1-9.
- [34] W. Li, F. Auger, Z. Zhang, and X. Zhu., Self-matched extracting wavelet transform and signal reconstruction, *Dig. Signal Process.* 128 (2022) 103602.
- [35] X. Zhu, Z. Zhang, J. Gao., Three-dimension extracting transform, *Signal Process.* 179 (2021) 107830.
- [36] D. He, H. Cao, S. Wang, and X. Chen, Time-reassigned synchrosqueezing transform: the algorithm and its applications in mechanical signal processing, *Mech. Syst. Signal Process.*, 117 (2019) 255-279.

- [37] G. Yu., A concentrated time-frequency analysis tool for bearing fault diagnosis, *IEEE Trans. Instrum. Meas.* 69 (2) (2019) 371-381.
- [38] W. Li, Z. Zhang, F. Auger, and X. Zhu., Theoretical analysis of time-reassigned synchrosqueezing wavelet transform, *Appl. Math. Lett.* 132 (2022) 108141.
- [39] W. Li, Z. Zhang, F. Auger, and X. Zhu., Time-extracting wavelet transform for characterizing impulsive-like signals and theoretical analysis, *Circuits, Systems, and Signal Processing* <https://doi.org/10.1007/s00034-022-02253-7>.
- [40] D. Fourer, F. Auger, Second-order time-reassigned synchrosqueezing transform: application to draupner wave analysis, in: *EUSIPCO 2019, Coruna, Spain*, pp. 1-11, doi: 10.23919/EUSIPCO.2019.8902342.
- [41] Z. He, X. Tu, W. Bao, Y. Hu and F. Li, Gaussian-modulated linear group delay model-application to second-order time-reassigned synchrosqueezing transform, *Signal Process.*, 167 (2020) 107275.
- [42] Z. He, X. Tu, W. Bao, Y. Hu and F. Li., Second-order transient-extracting transform with application to time-frequency filtering, *IEEE Trans. Instrum. Meas.* 69 (8) (2020) 5428-5437.
- [43] G. Yu, T. R. Lin., Second-order transient-extracting transform for the analysis of impulsive-like signals, *Mech Syst. Signal Process.* 147 (2021) 107069.
- [44] J. M. Lilly, and S. C. Olhede, On the analytic wavelet transform, *IEEE Trans. Info. Theo.* 56 (8) (2010) 4135-4156.
- [45] D.R. Smart, *Fixed point theorems*, Cambridge University Press, Cambridge, (1980).
- [46] I. Daubechies, Y. Wang, and H.T. Wu, ConceFT: concentration of frequency and time via a multi-tapered synchrosqueezed transform, *Philos. Trans. R. Soc.* 374 (2065) (2016) 20150193.
- [47] E. Sejdić, I. Djurović, and L. Stanković, Quantitative Performance Analysis of Scalogram as Instantaneous Frequency Estimator. *IEEE Transactions on Signal Processing.* 56 (8) (2008) 3837-3845.